4

# Semiannual Technical Report

## Pseudomorphic Semiconducting Heterostructures from Combinations of AlN, GaN and Selected SiC Polytypes: Theoretical Advancement and its Coordination with Experimental Studies of Nucleation, Growth, Characterization and Device Development

Supported under Grant #N00014-90-J-1427
Office of the Chief of Naval Research
Report for the period 7/1/94–12/31/94



R. F. Davis, S. Kern, K. Linthicum, R. Patterson, S. Tanaka and V. Torres
Materials Science and Engineering Department
North Carolina State University
Campus Box 7907
Raleigh, NC 27695-7907



December, 1994

# REPORT DOCUMENTATION PAGE

*Form Approved*
*OMB No. 0704-0188*



| 1. AGENCY USE ONLY *(Leave blank)* | 2. REPORT DATE | 3. REPORT TYPE AND DATES COVERED |
|---|---|---|
| | December, 1994 | Semiannual Technical 7/1/94–12/31/94 |

**4. TITLE AND SUBTITLE**

Pseudomorphic Semiconducting Heterostructures from Combinations of AlN, GaN and Selected SiC Polytypes: Theoretical Advancement and its Coordination with Experimental Studies of Nucleation, Growth, Characterization and Device Development

**5. FUNDING NUMBERS**

414s007---01
1114SS
N00179
N66005
4B855

**6. AUTHOR(S)**

Robert F. Davis

**7. PERFORMING ORGANIZATION NAME(S) AND ADDRESS(ES)**

North Carolina State University
Hillsborough Street
Raleigh, NC 27695

**8. PERFORMING ORGANIZATION REPORT NUMBER**

N00014-90-J-1427

**9. SPONSORING/MONITORING AGENCY NAMES(S) AND ADDRESS(ES)**

Sponsoring: ONR, Code 314, 800 N. Quincy, Arlington, VA 22217-5660
Monitoring: Administrative Contracting Officer, Regional Office Atlanta
Regional Office Atlanta, 101 Marietta Tower, Suite 2805
101 Marietta Street
Atlanta, GA 30332-0490

**10. SPONSORING/MONITORING AGENCY REPORT NUMBER**

**11. SUPPLEMENTARY NOTES**

**12a. DISTRIBUTION/AVAILABILITY STATEMENT**

Approved for Public Release; Distribution Unlimited

**12b. DISTRIBUTION CODE**

**13. ABSTRACT** ***(Maximum 200 words)***

Beta(3C)-SiC nucleation and 2H-SiC step flow growth have been achieved on 2H-AlN thin film templates using gas-source (GS) MBE and $C_2H_4/Si_2H_6$ gas flow ratios of 1 and 5, respectively. In addition, thin epitaxial films of AlN and SiC/AlN multilayers have been grown by plasma-assisted, GSMBE at 1050°C using $Si_2H_6$, $C_2H_4$ and $N_2$. RHEED and high-resolution TEM revealed monocrystalline layers and pseudomorphic interfacial relationships at the substrate/film and the film/film interfaces. X-ray rocking curve measurements on the (0002) Bragg peak of the AlN films indicate they are the highest quality ever reported. Auger spectroscopy, TEM and electron energy loss spectroscopy have been used to show that the solid solublilty between AlN and SiC is very limited below 1950°C. Results regarding the high temperature growth and the use of graded buffer layers for optimizing the microstructural quality of GaN grown by ECR-assisted GSMBE is also reported. The use of supersonic jets (SSJ) to produce GaN thin films has also been incorporated into this program. Highly oriented wurtzite GaN(001) films were grown on sapphire(0001) in the temperature range of 500°C to 650°C by SSJ. The film growth was controlled by the decomposition rate of $NH_3$. Growth rates as high as 4.5 μm/hr were achieved. The films had a columnar morphology.

| 14. SUBJECT TERMS | 15. NUMBER OF PAGES |
|---|---|
| pseudomorphic, beta-SiC, 2H-SiC, AlN, thin films, RHEED, TEM, X-ray rocking curve, graded layers, AlN-SiC solid solutions, chemical interdiffusion, equilibrium, supersonic jets | 39 |
| | 16. PRICE CODE |

| 17. SECURITY CLASSIFICATION OF REPORT | 18. SECURITY CLASSIFICATION OF THIS PAGE | 19. SECURITY CLASSIFICATION OF ABSTRACT | 20. LIMITATION OF ABSTRACT |
|---|---|---|---|
| UNCLAS | UNCLAS | UNCLAS | SAR |

# Table of Contents

# I. Introduction

The advent of techniques for growing semiconductor multilayer structures with layer thicknesses approaching atomic dimensions has provided new systems for both basic physics studies and device applications. Most of the research involving these structures has been restricted to materials with lattice constants that are equal within $\simeq 0.1\%$. However it is now recognized that interesting and useful pseudomorphic structures can also be grown from a much larger set of materials that have lattice-constant mismatches in the percent range. Moreover, advances in computer hardware and software as well as the development of theoretical structural and molecular models applicable for strained layer nucleation, growth and property prediction have occurred to the extent that the field is poised to expand rapidly. It is within this context that the research described in this report is being conducted. The materials systems of concern include combinations of the direct bandgap materials of AlN and GaN and selected, indirect bandgap SiC polytypes.

The extremes in thermal, mechanical, chemical and electronic properties of SiC allow the types and numbers of current and conceivable applications of this material to be substantial. However, a principal driving force for the current resurgence of interest in this material, as well as AlN and GaN, is their potential as hosts for high power, high temperature microelectronic and optoelectronic devices for use in extreme environments. The availability of thin film heterostructural combinations of these materials will substantially broaden the applications potential for these materials. The pseudomorphic structures produced from these materials will be unique because of their chemistry, their wide bandgaps, the availability of indirect/direct bandgap combinations, their occurrence in cubic and hexagonal forms and the ability to tailor the lattice parameters and therefore the amount of strain and the physical properties via solid solutions composed of the three components.

The research conducted in this reporting period and described in the following sections has been concerned with (1) the growth of beta(3C)- and 2H-SiC films on 2H-AlN thin film templates via gas source MBE, (2) the deposition of epitaxial films of AlN and SiC/AlN multilayers on 6H-SiC wafers, (3) the study of these layers and their pseudomorphic interfacial relationships via TEM, (4) the chemical interdiffusion and the question of the extent of equilibrium solid solution in the AlN-SiC system, (5) the use of $Al_XGa_{1-X}$ graded buffer layers to optimize the structural and microstructural quality of GaN films and (6) the use of supersonic jets to successfully deposit GaN films.

These sections detail the procedures, results, discussions of these results, conclusions and plans for future research. Each subsection is self-contained with its own figures, tables, and references.

## II. Growth of 2H-Silicon Carbide using Pseudomorphic 2H-Aluminum Nitride Layer on 6H-Silicon Carbide Substrates by Gas-source Molecular Beam Epitaxy

### A. Introduction

High purity, monocrystalline silicon carbide (SiC) is being extensively studied for high-temperature, -power and -frequency electronic device applications [1]. More than 250 polytypes or stacking arrangements of the closest packed Si/C bilayers along the crystallographic axes of closest packing have been reported [2]. The 3C or β, 15R, 6H and 4H polytypes are the most common; the numerals and the letters refer to the number of bilayers needed to form a unit cell and the cubic or hexagonal nature of the cell, respectively. 3C and 6H films has been grown successfully by many researchers [3]. Another polytype, 2H, has also been desired for electronic device applications because it has the largest band gap of any SiC polytype (3.3 eV) and a higher electron mobility than 6H and 15R [4]. However, deposition of the 2H polytype has been unsuccessful until recently, and then only in the form of small whiskers [4-7]. Recently, NASA's group has reported the first successful growth of 2H-SiC films on 6H-SiC substrates by pulsed laser ablation [8]. The structural study using transmission electron microscopy (TEM) showed the symmetry of a film grown at 1270°C as c-axis oriented 2H-SiC containing columnar grains with average diameter of 20 nm and length of 100 nm.

In general, films having the same polytypes as the substrate can be deposited, if the growth mode is 'step flow.' Step flow can be achieved kinetically when the deposited adatoms reach surface step sites and retain the identical stacking sequence as the substrate. Thus, 6H films can be formed on 6H(0001) substrates with the availability of steps even at growth temperatures <1500°C, i.e., in the temperature regime where 3C is found by experiment [2] to be the more commonly deposited phase (although quantum mechanical calculation [9] predicts 6H to be more stable than 3C). The steps serve as the primary surface template which forces replication of the substrate polytype in the growing film. Step flow has been achieved experimentally via CVD in the homoepitaxial growth of 6H and 4H films between 1200 and 1600°C [3, 10, 11]. By contrast, previous SiC film growth studies via MBE at lower growth temperatures (<1200°C) on 6H-SiC substrates did not result in step flow and homoepitaxial reproduction of the 6H substrate. Recently, however, we have successfully achieved step flow growth and even control of polytypes by changing the gas flow ratio of $C_2H_4/Si_2H_6$ [12]. The problem in growing 2H-SiC film is potentially the lack of 2H-SiC substrates. Since AlN has the wurtzite (2H) structure and is closely lattice matched to SiC, this material may be used as a template of the 2H structure to achieve our goal.

In this study, we have investigated the possibility of forming the 2H-SiC and growing SiC by step flow under certain growth conditions on a 2H-AlN which is grown on 6H-SiC substrates by plasma-assisted(PA) GSMBE [13]. Under the ethylene rich conditions, i. e., the gas flow ratio of $C_2H_4/Si_2H_6 = 5$, we have observed the formation of 2H-SiC on 2H-AlN. It should, however, be noted that since the film of 2H-SiC was very thin, further investigations is necessary to confirm this result.

B. Experimental Procedure

The very thin, ~15 Å, AlN films were first grown via PAGSMBE on the Si(0001) surfaces of either vicinal (3-4° off from (0001) toward <11$\bar{2}$0>) or on-axis α(6H)-SiC substrates. A detailed description of the deposition technique has been published [14]. After the growth of AlN films followed by taking RHEED patterns, SiC films were deposited under the various conditions given in Table I. Following growth and RHEED observation, each sample was cut and glued face-to-face and thinned to electron transparency using standard cross-sectional TEM preparation techniques [15]. Each sample was examined along the <$\bar{2}$110> zone axis using a Topcon EM-OO2B operated at a 200kV acceleration voltage.

Table I. Range of growth conditions for the SiC films

| | |
|---|---|
| Substrate | 2H-AlN/6H-SiC |
| Temperature | 1050 °C |
| $Si_2H_6$ flow rate | 0.1 sccm |
| $C_2H_4$ flow rates | 0.1, 0.5 sccm |
| $C_2H_4/Si_2H_6$ flow rate ratios | 1.0, 5.0 |
| Growth rates and time | ≈10-50 Å/hr, 1 hr. |

C. Results

Figure 1 shows a cross-sectional TEM micrograph of the multi-layer structure including 3C-SiC, 2H-AlN, and 6H-SiC substrate. The top SiC layer was grown at the gas flow ratio ($C_2H_4/Si_2H_6$) of 1. Island-like 3C-SiC is evident on 2H-AlN thin film, which is ~15 Å in thickness. It should be noted that under the same condition as used in this film growth step flow is occurred on 6H-SiC substrate because of (3×3) surface reconstruction according to our recent study [12]. This implies that nucleation of 3C phase is enhanced probably by the presence of Al- or N- dangling bonds on the AlN(0001) surface. Either Si or C adatoms (molecules) may reduce their diffusion lengths on the AlN surface and thus very small numbers of adatoms might reach the step sites where crystallographic information of 2H structure can only be supplied.

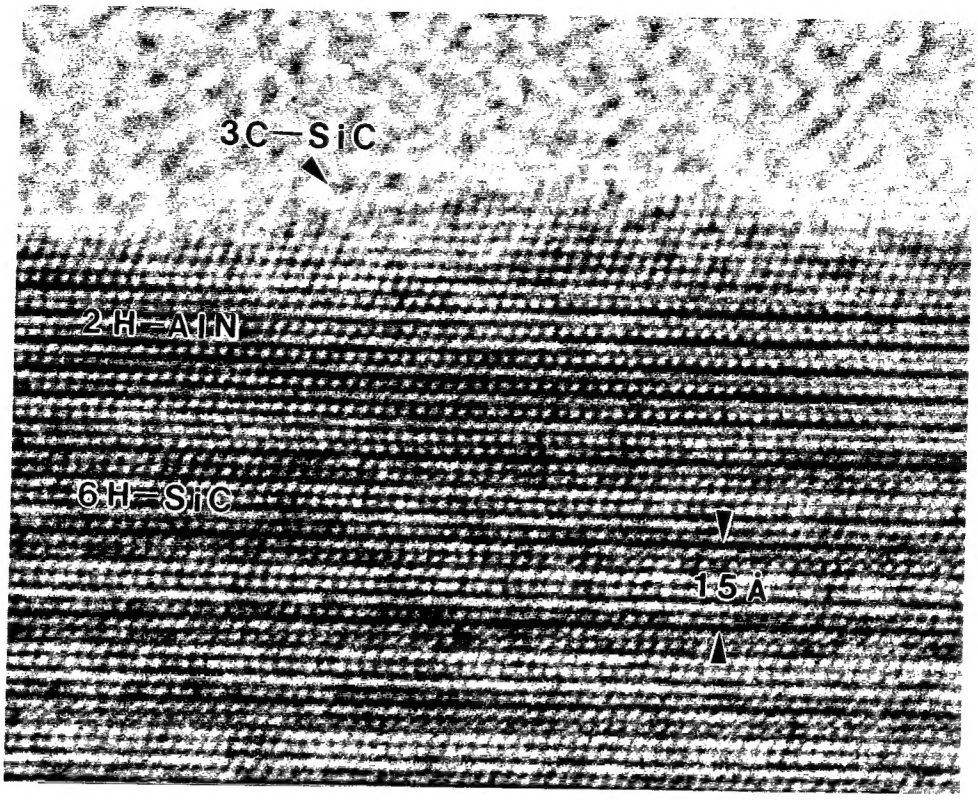


Figure 1. HRTEM image of the multi-layer structure of 3C-SiC/2H-AlN/6H-SiC. The SiC film was grown at the gas flow ratio of 1.

In contrast, no 3C region can be observed in the sample which was grown at the gas flow ratio ($C_2H_4/Si_2H_6$) of 5, as seen in Fig. 2. Surface morphology appeared to be step flow pattern. The film thickness of SiC, however, is too small to clearly discern the SiC layer. Our preliminary investigation of SiC film growth on 6H-SiC substrate indicated the presence of SiC film under more ethylene-rich conditions and that the growth rates of SiC film on AlN and SiC surfaces were comparable. In combing these results, the presence of 2H-SiC layer is plausible. Further experiments are necessary to elucidate this problem.

D. Discussion

The gas flow ratio of $C_2H_4/Si_2H_6$ was found to affect polytypes of SiC films on the 2H-AlN(0001) surfaces. Under equal flow rates of each gas the 3C nuclei and island-like surface morphology was observed. In contrast, ethylene-rich condition might give rise to 2H polytype of SiC on the 2H-AlN surfaces. The change in polytypes under the two different growth conditions should be discussed in terms of surface chemistry of AlN(0001) and bonding configurations of SiC/AlN interface including step sites.

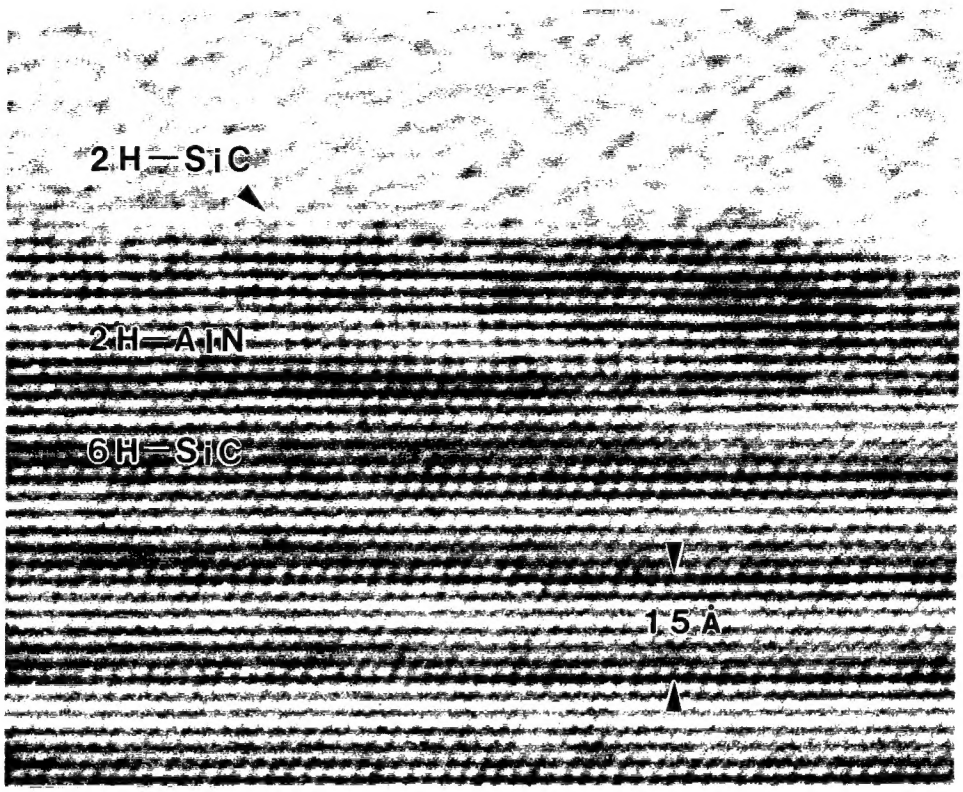


Figure 2. HRTEM image of the multi-layer structure of 2H-SiC/2H-AlN/6H-SiC. The SiC film was grown at the gas flow ratio of 5. The thickness of 2H-SiC is ~2-3 bilayers.

AlN(0001) surface is assumed to be Al-terminated because the 6H-SiC substrate used in this study was Si face on which preferentially formed Si-N bonding at the AlN/6H-SiC interface[16]. Thus, there are Al dangling bonds on the AlN surface except at the step sites, which may possess N dangling bonds, as indicated in Fig. 3. An energetic calculation [16] predicts that adatoms (molecules) of Si and C species react the AlN surface to form either Si-N and C-Al bonds, respectively. The Al-Si bond is rather unfavorable in the calculation, however, under the gas flow ratio (R) of 1 it may be created kinetically to form 3C nuclei on the terrace sites, as was observed in Fig. 1. On the other hand, majority of $C_2H_4$ gas molecules at R = 5 may cover the Al dangling bonds by forming C-Al bonding configuration which hinder the formation of 3C nuclei on the terrace sites. $Si_2H_6$ molecules can reach the step site and form Si-N bond to retain the same stacking sequence of 2H-AlN. It should be noted here that 2H retention is only possible at step sites and 3C nucleation occurs on terrace sites due to thermodynamic point of view.

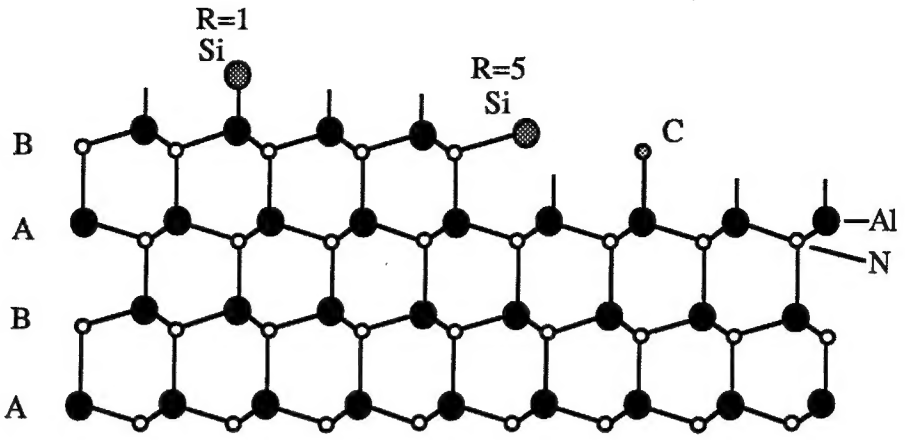


Figure 3. AlN surface structure.

E. Conclusion

2H polytype of SiC film has been kinetically stabilized on very thin 2H-AlN thin films, which were pseudomorphically deposited on 6H-SiC substrates. The AlN thin layer plays a role as a template of 2H structure. Under the different gas flow ratios of $C_2H_4/Si_2H_6$ during SiC growth the difference in polytypes of SiC films have been observed. Ethylene-rich condition is considered to kinetically stabilize the 2H-SiC structure at the growth temperature of 1050°C mainly due to prevention of 3C nuclei on the terrace sites by C-Al bondings. The detailed mechanisms of 3C nucleation on the terrace sites is still unknown, however, it is probably related to Si-Al bonding characteristics.

F. Future Plans

The strong evidence for the presence of 2H-SiC is desired. Several attempts should be made to grow thicker 2H-SiC in the same experimental methods. Based on the previous study including the growth mechanism of SiC film on 6H-SiC substrate [12], thicker 2H-SiC will probability be deposited on very thin 2H-SiC layer obtained in this experiment using the gas flow ratio of 1, which enhances step flow. Dependence of growth temperature of SiC will also be studied.

G. References

1. R. F. Davis, Physica B **185**, 1 (1993).
2. N. W. Jepps and T. F. Page, Progress in Crystal Growth and Characterization vol. 7, edited by P. Krishna (Pergamon Press, New York, 1983), 259.
3. For example see, H. S., Kong, J. T. Glass, and R. F. Davis, J. Appl. Phys.**64**, 2672 (1988).
4. L. Patrick, J. Appl. Phys. **37**, 4911 (1966).
5. R. F. Adamsky and K. M. Merz, Z. Krist. **111**, 350 (1959).

6. M. I. Sokhor and V. P. Glukhov, Sov. Phys. Crystallogr. **10**, 341 (1963).
7. J. A. Powell, J. Appl. Phys. **40**, 4660 (1969).
8. M. A. Stan, M. O. Patton, and J. D. Warner, Appl. Phys. Lett. **64**, 2667 (1994).
9. V. Heine, C. Chen, and R. J. Needs, J. Am. Ceram. Soc. **74**, 2630 (1991).
10. H. Matsunami, T. Ueda, and H. Nishino, Mater. Res. Soc. Symp. Proc. **162**, 397 (1990).
11. L. B. Rowland, R. S. Kern, S. Tanaka, and R. F. Davis, J. Mater. Res. **8**, 2753 (1993).
12. S. Tanaka, R. S. Kern, and R. F. Davis, Appl. Phys. Lett., to be published in Nov. 28 (1994).
13. S. Tanaka, R. S. Kern, and R. F. Davis, Appl. Phys. Lett., to be published in Jan. 3 (1995).
14. L. B. Rowland, R. S. Kern, S. Tanaka, and R. F. Davis, J. Mater. Res. **8**, 2310 (1993).
15. C. H. Carter, Jr., R. F. Davis, and S. R. Nutt, J. Mater. Res. **1**, 811 (1986).
16. W. R. L. Lambrecht and B. Segall, Phys. Rev. B **43**, 7070 (1991).

# III. Characterization of AlN and AlN-SiC Pseudomorphic Heterostructures on α(6H)-SiC(0001) Grown by Plasma-assisted, gas-source Molecular Beam Epitaxy

## A. Introduction

A marked increase in the interest in wide band gap semiconductor materials for use in high-temperature, -power, -frequency and -speed microelectronic devices resistant to radiation and short-wavelength optoelectronic devices has recently been demonstrated on a global scale. Two candidate materials that have generated much of this interest are SiC and AlN. SiC, the only binary compound in the Si-C system, forms in many different polytypes; the most common being the only cubic polytype, β- or 3C-SiC, and one of the hexagonal polytypes, 6H-SiC. Since the band gap for SiC (3.0 eV for 6H and 2.3 eV for 3C) is indirect, it cannot be used alone for optoelectronic applications. For this reason, AlN, with its direct band gap of 6.28 eV, is of particular interest for use with SiC. Two methods of simultaneously exploiting the favorable characteristics of these materials include the thin film deposition of both pseudomorphic heterostructure and alloys.

Aluminum nitride possesses a direct band gap of 6.28 eV at 300 K [1], a melting point in excess of 2275 K [2] and a thermal conductivity of 3.2 W/cm·K [3]. As such, it is a candidate material for high-power and high-temperature microelectronic and optoelectronic applications with the latter employment being particularly important in the ultraviolet region of the spectrum[1]. This material also has the highest reported surface acoustic wave velocity (Raleigh $V_R$=6–6.2 km/s, $V_L$=11-12 km/s [4]-[6]) for any material and a substantial electromechanical coupling coefficient (to 1% [7]). These properties strongly indicate that superior surface acoustic wave devices, operational in aggressive media and under extreme conditions both as sensors for high temperatures and pressures and as acousto-optic devices can be developed [8-10]. However, progress regarding these (and other) applications is hampered by the lack of good single crystal material. The primary objective of the research reported below has been to address this issue via the fabrication of thin films of this material via molecular beam epitaxy (MBE) techniques.

In previous studies, mono- and polycrystalline films of AlN have been grown by chemical vapor deposition (CVD) using $NH_3$ and $Al(CH_3)_3$ or $AlCl_3$ on α(6H)-SiC [11], sapphire [1,9,12], and Si [13-15]. Chu *et al.* [11] obtained smooth monocrystalline AlN layers to a thickness of 25 μm on α(6H)-SiC{0001} substrates by chemical vapor deposition (CVD) from 1200-1250°C. A high density of defects in these AlN films was revealed by chemical etching. In general, films grown on sapphire and Si substrates possessed a much rougher morphology than those grown on α(6H)-SiC. This occurred very likely because the difference in lattice

parameters between AlN and SiC is substantially less than between AlN and sapphire or AlN and Si.

Gas source MBE using electron beam evaporated Al and $NH_3$ on Si(111) and $Al_2O_3$(0001) and (01$\bar{1}$2) at 1000-1200°C[16] or thermally evaporated Al and plasma-derived activated nitrogen species on α(6H)-SiC (0001) and $Al_2O_3$ (0001) at 600-1250°C[17,18] has also been used for single crystal AlN growth.

Pseudomorphic heterostructures of dissimilar semiconductor materials are the basis for quantum well and laser devices. The physical properties (e.g., lattice parameter, crystal structure, melting point and thermal expansion) as well as the optical and electronic properties (e.g., band gap and index of refraction) of SiC and AlN indicate that stable superlattice structures of these materials having the desired properties are feasible. Theoretical calculations regarding electronic structure and bonding at AlN/SiC interfaces [19] and critical layer thickness prior to misfit dislocation formation at interfaces in cubic AlN and SiC have been reported [20]. Rowland *et al.* [21] and Kern *et al.* [22] have described the growth of 3C-SiC/2H-AlN pseudomorphic layers on α(6H)-SiC(0001) substrates by plasma-assisted, gas-source molecular beam epitaxy (PAGSMBE) using solid Al evaporated from a standard effusion cell and the gas sources of $Si_2H_6$, $C_2H_4$ and $N_2$. The resulting SiC layers contained a high density of stacking faults and microtwins caused primarily by interfacial stresses and the low stacking fault energy intrinsic to β-SiC.

B. Experimental Procedure

In the present research, a specially designed and previously described [23] PAGSMBE system was employed to deposit all AlN-SiC thin films on the Si faces of α(6H)-SiC(0001) substrates. Both on-axis and off-axis (oriented $3.5 \pm 0.5°$ off (0001) toward [11$\bar{2}$0]) SiC substrates were used. The substrates were cleaned chemically before growth in a 10% HF solution for 5 minutes, and loaded immediately into the UHV growth chamber. Sources of Si and C were disilane ($Si_2H_6$, 99.99% purity) and ethylene ($C_2H_4$, 99.99% purity), respectively. Aluminum (99.9999% purity) was evaporated from a standard MBE effusion cell operated in all cases at 1260°C. A compact electron cyclotron resonance (ECR) plasma source supplied by ASTeX, Inc., operating at 100 W forward power, was used to decompose $N_2$ (99.9995% purity). All AlN layers were grown at with the Al effusion cell operating at 1260°C and the ECR at 100W forward power with 3.5 sccm $N_2$. Typical gas flow rates employed for SiC growth for use in heterostructures were 0.1-2.0 sccm $Si_2H_6$, 0.1-2.0 sccm $C_2H_4$ (Si/C ratio was kept at 1/1). Individual layers of SiC and AlN were grown for variable times ranging from 30 seconds to 5 hours. All layers were grown at 1050°C.

Reflection high-energy electron diffraction (RHEED) at 10 kV and high-resolution transmission electron microscopy (HRTEM) were used for structure and microstructure

analyses. Samples were prepared for HRTEM using standard techniques[7]. A Topcon EM 002B high-resolution transmission electron microscope was used at 200 kV for the HRTEM analysis. X-ray rocking curve measurements were made on a double crystal diffractometer at Brown University by Drs. F. R. Chien and S. R. Nutt. Secondary ion mass spectrometry (SIMS), using a Cameca IMS-3f ion microprobe operating at 10 keV with $Cs^+$ ions, was employed to determine the atomic concentration of impurities. Carrier concentrations for undoped SiC films, grown on insulating AlN layers, were measured at room temperature by standard Hall techniques at 3.5 kG. Nickel contacts, RF sputtered at room temperature then annealed at 1000°C for 30 s in Ar, were used on the undoped and films.

C. Results

*Aluminum Nitride*. Figure 1 shows an x-ray rocking curve of a 2H-AlN/6H-SiC structure grown on vicinal α(6H)-SiC(0001) at 1050°C. The AlN layer is approximately 0.75 μm thick. The graph shows the $(0006)_{SiC}$ and the $(0002)_{AlN}$ Bragg reflections as determined by a double crystal x-ray diffractometer. The full-width half maximum (FWHM) of the AlN peak is 43.2 arc sec. Figure 2 shows an x-ray rocking curve of the same 2H-AlN/6H-SiC structure grown on on-axis α(6H)-SiC(0001) at 1050°C. In this case, the AlN layer is also approximately 0.75 μm thick. The full-width half maximum of the $(0002)_{AlN}$ Bragg reflection peak is 80 arc sec.

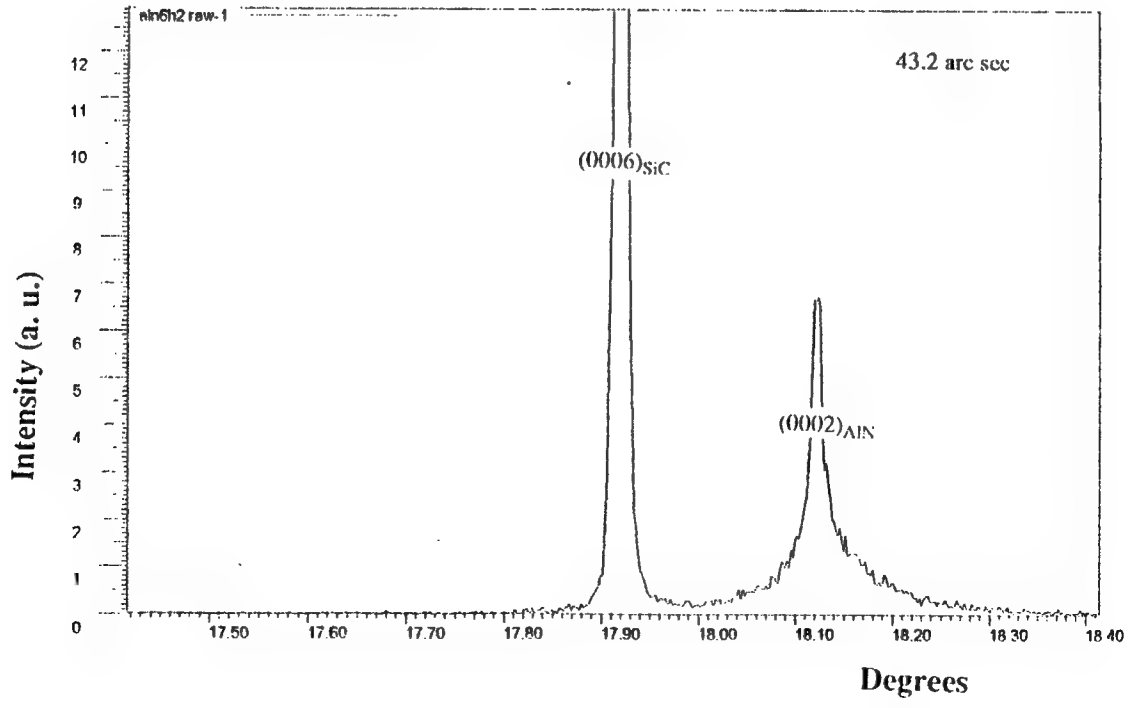


Figure 1. X-ray rocking curve of a 2H-AlN layer grown on vicinal 6H-SiC(0001).

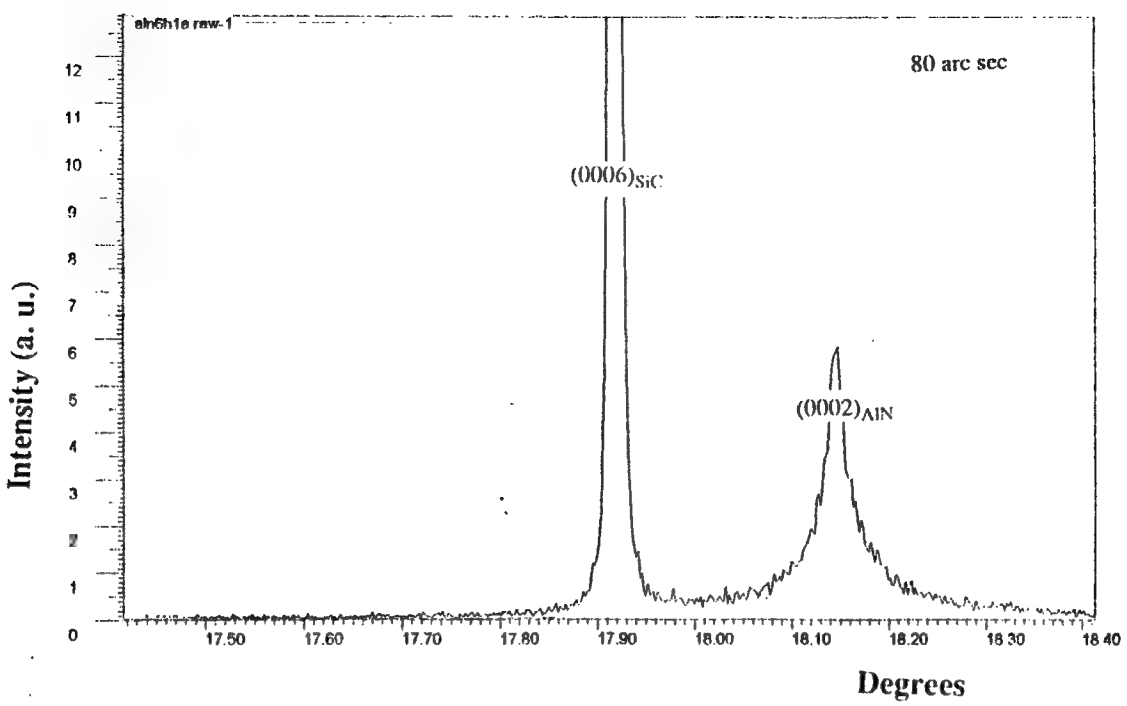


Figure 2. X-ray rocking curve of a 2H-AlN layer grown on on-axis 6H-SiC(0001).

*AlN/SiC Heterostructures*. Undoped films of β-SiC(111) have been grown on thin, insulating layers of 2H-AlN(0001) similar to the structure shown in Fig. 3 at 1050°C using 1.0 sccm $Si_2H_6$ and 1.0 sccm $C_2H_4$. Growth rates approaching 1000 Å per hour were achieved. Hall electrical measurements made on some of the thicker SiC films (≈0.75 μm) have showed the films to be n-type with electron concentrations as low as $3\times10^{15}$ $cm^{-3}$ and mobilities as high as 648 $cm^2V^{-1}s^{-1}$.

*AlN Doping*. Preliminary attempts to dope AlN with Si (using $Si_2H_6$) and C (using $C_2H_4$) have been undertaken. Secondary ion mass spectroscopy analysis has shown that controllable levels of Si and C can be incorporated into AlN at very constant concentrations. However, the resulting films contained measurable levels of O despite no evidence of water or oxygen in the chamber as measured by a Residual Gas Analyzer (Leybold-Inficon Model H100M). Since standards for these elements in AlN were not available, no quantitative measurements were made. All attempts to measure these samples by the Hall technique were unsuccessful due to the extremely insulating nature of these films.

D. Discussion

In both Figs. 1 and 2, the x-ray rocking curve measurements represent the best values reported by any previous researchers. Curiously, films grown on the vicinal substrates, which

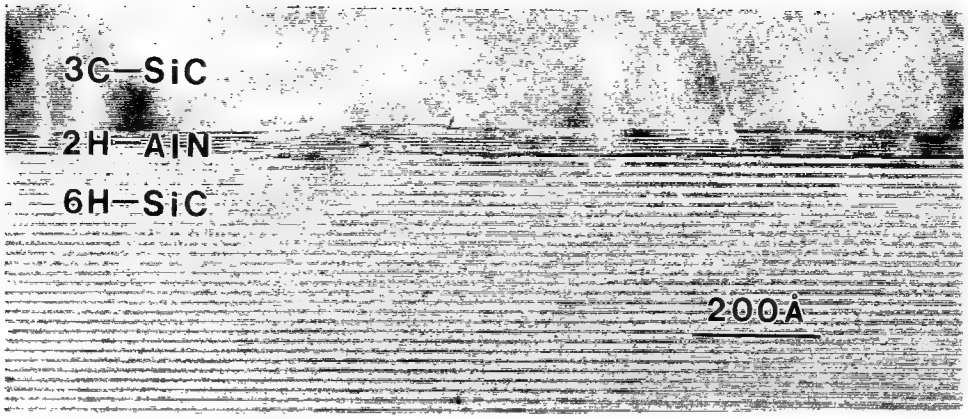


Figure 3. HRTEM micrograph of a SiC/AlN multilayer grown on on-axis 6H-SiC(0001). Electrical characterization of the similar β-SiC(111) layers has been done.

have previously been demonstrated to have rougher surfaces and higher defect densities, have lower value of FWHM for the (0002) Bragg reflection. Previous reports have shown that defects are created in the vicinity of the steps in the vicinal substrates. These defects may play a role in stress relief and contribute to the lower measured values of FWHM.

The results of the Hall measurements on undoped β-SiC, grown on AlN on on-axis 6H-SiC, represent some of the lowest unintentional doping levels ever reported in the cubic polytype. It may be possible to lower these values by more efficient removal from the system of $N_2$ which makes up the largest mole fraction of the gas present in the chamber prior to SiC growth after the AlN deposition.

Early results in AlN doping have been unsuccessful in creating conducting layers. The presence of measurable quantities of O in the films may be indicative of a problem with the ECR source[24]. In this report, the investigators believe that the ECR source, which has a quartz liner in the vicinity of the plasma, may be the source of Si and O in their GaN films due to erosion of the liner.

## E. Conclusions

Monocrystalline layers of AlN as well as heterostructures of AlN and SiC have been grown by PAGSMBE on on-axis and vicinal α(6H)-SiC(0001) substrates. X-ray rocking curve measurements have been made on the AlN layers on vicinal and on-axis 6H-SiC(0001) and have resulted in values of 43.2 and 80 arc sec, respectively. Undoped, cubic SiC(111) layers have been measured electrically and have revealed carrier concentration as low as $3\times10^{15}$ $cm^{-3}$ and mobilities as high as 648 $cm^2V^{-1}s^{-1}$. Preliminary attempts to dope AlN have been attempted but are inconclusive at this time.

F. Future Plans and Goals

Further studies into the growth and doping of these materials in planned. In addition, several experiments are planned to try to optimize the source of N used in this research. The first of these is to replace the quartz liner in the existing ECR source with a liner made of pBN. A cooperative effort between NCSU and ASTeX is currently being discussed in an attempt to resolve this situation. Ammonia is also a potential source of N being considered and planned for testing.

G. References


1. W. M. Yim, E. J. Stofko, P. J. Zanzucchi, J. I. Pankove, M. Ettenberg, and S. L. Gilbert, J. Appl. Phys. **44**, 292 (1973).
2. M. G. Norton, B. C. H. Steele, and C. A. Leach, Science of Ceramics, **14**, 545 (1988).
3. G. A. Slack, J. Phys. Chem. Solids **34**, 321 (1973).
4. M. Kitayama, T. Fukui, T. Shiosaki, and A. Kawabata, Japan J. Appl. Phys. **22**, 139 (1982).
5. G. R. Kline and K. M. Lakin, Proc. IEEE Symp. Ultrasonics **14**, 495 (1983).
6. K. Tsubouchi, K. Sugai, and N. Mikoshiba, Proc. IEEE Symp. Ultrasonics **14**, 340 (1983).
7 M. Sano and M. Aoki, Oyo Butsuri, **52**, 374 (1983).
8. J. K. Liu, K. M. Lakin, and K. L. Wang, J. Appl. Phys **46**, 3703 (1975).
9. M. Morita, N. Uesugi, S. Isogai, K. Tsubouchi, and N. Mikoshiba, Jpn. J. Appl. Phys. **20**, 17 (1981).
10. G. D. O'Clock, Jr. and M. T. Duffy, Appl. Phys. Lett. **23**, 55 (1973).
11. T. L. Chu, D. W. Ing, and A. J. Norieka, Solid State Electron. **10**, 1023 (1967).
12. H. M. Manasevit, F. M. Erdmann, and W. I. Simpson, J. Electrochem. Soc. **118**, 1864 (1971).
13. M. Morita, S. Isogai, N. Shimizu, K. Tsubouchi, and N. Mikoshiba, Japan. J. Appl. Phys. **20**, L173 (1981).
14. Z. J. Yu, J. H. Edgar, A. U. Ahmed, and A. Rys, J. Electrochem. Soc. **138**, 196 (1991).
15. A. J. Noreika and D. W. Ing, J. Appl. Phys. **19**, 5578 (1968).
16. S. Yoshida, S. Mizawa, Y. Fujii, S. Takada, H. Hayakawa, S. Gonda, and A. Itoh, J. Vac. Sci. Technol. **16**, 990 (1979).
17. Z. Sitar, M. J. Paisley, B. Yan, R. F. Davis, J. Ruan, and J. W. Choyke, Thin Solid Films **200**, 311 (1991).
18. L. B. Rowland, R. S. Kern, S. Tanaka and R. F. Davis, J. Mater. Res. **8**, 2310 (1993).
19. W. R. L. Lambrecht and B. Segall B, Phys. Rev. B **43**, 7070 (1991).
20. M. E. Sherwin and T. J. Drummond, J. Appl. Phys. **69**, 8423 (1991).
21. L. B. Rowland, R. S. Kern, S. Tanaka and R. F. Davis, Appl. Phys. Lett. **62**, 3333 (1993).
22. R. S. Kern, S. Tanaka, and R. F. Davis, in *Proceedings of the International Conference on Sicon Carbide and Related Materials.*, ed. by M. G. Spencer, R. P. Devaty, J. A. Edmond, M. A. Khan, R. Kaplan and M. Rahman (Institute of Physics Publishing, Bristol, UK, 1994), pp. 389–392.
23. L. B. Rowland, R. S. Kern, S. Tanaka, and R. F. Davis, in *Proceedings of the Fourth International Conference on Amorphous and Crystalline Silicon Carbide*, edited by C. Y. Yang, M. M. Rahman, and G. L. Harris (Springer-Verlag, Berlin, 1992), p. 84-89.
24. R. J. Molnar and T. D. Moustakas, J. Appl. Phys. **76**, 4587 (1994).

# IV. Chemical Interdiffusion between α(6H)SiC (0001) and Monocrystalline AlN Thin Films

## A. Introduction

One compound which has been reportedly alloyed with α(6H)-SiC ($a_o$ = 3.08Å) is AlN ($a_o$ = 3.11Å) due to the similarities in the atomic and covalent radii and the crystal structures. Diverse processing routes have been employed to achieve partial or complete solid solutions from these two compounds including reactive sintering or hot pressing of powder mixtures and thin film deposition from the vapor phase. There exists, however, a difference in opinion among investigators regarding the occurrence and the extent of solid solutions in the SiC-AlN system at T < 2100°C. Representative examples of these opinions are presented below.

Schneider *et al.*[1] concluded that the formation of $(AlN)_x(SiC)_{1-x}$ solid solutions were not favorable within the temperature range of his study of the AlN-$Al_4C_3$-SiC-$Si_3N_4$ system. He found two phase mixtures rather than $(AlN)_x(SiC)_{1-x}$ solid solutions when equal molar ratios of either SiC and AlN or $Si_3N_4$ and $Al_4C_3$ were hot pressed at 1760°C - 1860°C for 45 and 30 minutes, respectively. Ruh and co-workers [2-4] obtained no SiC-AlN solid solution for temperatures <2100°C and concentrations of ~35 to 100 mol % AlN using dry mixtures of SiC and AlN powders, hot-pressed in vacuum under the conditions of 35 MPa and 1700°C 2300°C In contrast, Rafaniello *et al.* [5] reported solid solutions as indicated by X-ray diffraction in samples hot-pressed at 1950°C - 2300°C and 70 MPa for ~3 h in Ar. However, using a more careful analysis of his X-ray diffraction data, Rafaniello and his colleagues subsequently showed [6] that the broadening of the SiC-AlN peak was caused by the existence of a two-phase region and not the 2H solid solution reported in [5]. The initial confusion was caused by the closeness (~1%) in the lattice parameters of SiC and AlN. This was supported by optical micrographs of multiphase assemblages in the sintered samples for temperatures as high as 2300°C. Rafaniello *et al.* [6] also revealed strong evidence of a miscibility gap by the precipitation of SiC-rich phase from 75 wt % AlN solid solution and precipitation of an AlN-rich phase from a 47 wt % AlN alloy, when hot-pressed samples were annealed at 1700°C for 90 h.

In contrast to the studies described above are reports of the formation of solid solutions between SiC and AlN at relatively low processing temperatures (i.e. within the proposed miscibility gap region). Cutler [7] formed solid solutions between SiC and AlN from 2 mol % -100 mol % AlN with a single wurtzite type phase, as determined by X-ray diffraction. This was accomplished by the carbothermal reduction of fine amorphous silica ('cabosil'), precipitated aluminum hydroxide, and a carbon source of starch/sugar in a nitrogen atmosphere at 1400°C - 1600°C. In subsequent work by Rafaniello [5], intimate mixtures of $SiO_2$, $Al_2O_3$ and C were reacted at 1650°C for 4 h in flowing $N_2$. Solid solutions over the entire composition range were reported.

Theoretical calculations of the immiscibility region in the $(AlN)_x(SiC)_{1-x}$ system were conducted by Sukhanek [8] using the dielectric theory of $A^NB^{8-N}$ semiconductors. The theory relates changes in the band structure to the enthalpy of formation in semiconductors. He concluded that the formation of a continuous series of solid solutions of silicon carbide with aluminum nitride were possible above 1000 K. This was shown by Shimada [9] who hot pressed mixtures of SiC, $Si_3N_4$, AlN and $Al_3C_4$ powders at 1300°C - 1900°C and 3.0 GPa for 1 h and reported the formation of solid solutions by X-ray diffraction. Tsukuma [10] also sintered mixtures of $Si_3N_4$ and $Al_4C_3$ in a gas autoclave at 1800°C and 10 MPa in argon. Solid solutions rich in AIN were produced. However, solutions in the SiC-rich region could not be formed under the same conditions.

It is clear that the atomic behavior and the extent of phase formation at relatively low temperatures < 2000° C for thin film deposition cannot be discerned from the research conducted previously. Likewise, the diffusivities of these species have not been studied for epitaxially deposited AIN on single crystal SiC. The purpose of this investigation has been to determine the extent of solid solution formation within the temperature range of 1700°-1950° C and to determine the diffusion mechanism, if any, that occurs.

B. Experimental Procedures

*Sample Preparation.* AlN/SiC diffusion couples were prepared using a modified Perkin-Elmer 430 molecular beam epitaxy (MBE) system and the conditions given in Table I. Aluminum (99.999%) was evaporated from a standard effusion cell. Activated nitrogen was achieved using an MBE compatible, electron cyclotron resonance plasma source. Single crystal AIN films having a thickness of ~1 μm and a low density of planar defects was epitaxially deposited on off-axis (3-4° toward [1110]) α(6H)-SiC(0001) wafers manufactured by Cree Research, Inc.

Table I. Growth Conditions for the 2H AlN Films on α(6H)-SiC(0001) Substrates

| | |
|---|---|
| Nitrogen pressure | $2\times10^{-4}$ Torr |
| Nitrogen flow rate | 4-5 sccm |
| ECR Microwave power | 50 W |
| Substrate temperature | 650° C |
| Growth rate | ~0.1 mm/hr |
| Total growth time | 7-8 hrs. |

Several different precautions were taken in order to prevent contamination of the samples and to minimize the loss of volatile components, principally aluminum, and nitrogen. The samples were placed in a high density pyrolitic graphite crucible. The inside of the crucible was previously coated with SiC by heating a mixture of Si and β-SiC powders inside the holder to 2000° C. The diffusion samples were placed inside this holder with the α(6H)-SiC(0001) face against the SiC coating. Bulk AIN squares were then placed on top of the deposited AIN. The holder was subsequently closed using a threaded lid.

Several different precautions were taken in order to prevent contamination of the samples and to minimize the loss of volatile components principally Al and N. The samples were placed in a high density pyrolitic graphite crucible. The inside of the crucible was previously coated with SiC by heating a mixture of Si and β-SiC inside the holder to 2000° C. The diffusion samples were placed inside this holder with the α(6H)-SiC(0001) face against the SiC coating. Bulk AIN squares were then placed on top of the deposited AIN. The holder was then closed using a threaded lid and loaded into the furnace. The chamber was evacuated ($2\times10^{-6}$ torr) to prevent contamination during diffusion. Nitrogen gas (99.9995%), purified by a gettering furnace containing heated Cu chips (Centorr Furnace model 2B-20) was then introduced into the chamber at a rate of 365 sccm. The chamber was brought to atmospheric pressure and a flowing $N_2$ environment maintained throughout each diffusion anneal. Diffusion temperatures were attained in ~20 min (exact value for 1850° C). The samples were then removed for characterization. The $N_2$ gas, bulk AIN and SiC coated crucible did not contibute to or hinder the diffusion. This was checked by a SiC-AlN standard which had not been annealed. The AIN as well as the SiC intensity in the standard were the same as AlN and SiC intensity outside of the diffused region. The samples were diffused within the ranges of temperature and time of 1700–1950°C and 10–70 h, respectively. A complete listing of temperatures and times are given in Table II.

The annealed couples were investigated chemically using depth profile Auger spectroscopy (AES) and parallel electron energy loss spectroscopy (PEELS) as well as microstructurally using transmission electron microscopy (TEM).

C. Results and Discussion

Table III indicates the approximate detection limits, calculated with a signal-to-noise ratio of 3, for the elements included in the multiplexed Auger data of the depth profile.

Atomic concentration was deduced from the peak-to-peak Auger signals for Al, N, Si, and C. Figures 1 and 2 show the depth profiles for samples 1 and 3, respectively.

Chemical analysis of regions from +70 A to -70 A from the interface showed no interdiffusion of any component. Table IV provides the results of PEELS analysis on both sides of the AlN/SiC interface.

Table II. Annealing Conditions used for the AlN/SiC Diffusion Couples

| | Temperature (°C) | Time (hrs) |
|---|---|---|
| Sample 5 | 1950 | 32 |
| Sample 3 | 1900 | 50 |
| Sample 1 | 1850 | 50 |
| | 1850 | 25 |
| | 1850 | 21.5 |
| | 1850 | 10 |
| | 1800 | 30 |
| | 1800 | 25 |
| | 1800 | 20 |
| | 1750 | 70 |
| | 1750 | 50 |
| | 1750 | 25 |
| | 1700 | 70 |
| | 1700 | 30 |

Table III. Approximate Auger Detection Limits for the Components of this Research

| Element | Elemental Sensitivity Factor | Detection Limit (at%) (10 kv) |
|---|---|---|
| Silicon | 0.042 | 2.3 |
| Carbon | 0.08 | 3.8 |
| Aluminum | 0.07 | 2.9 |
| Nitrogen | 0. 16 | 1.1 |

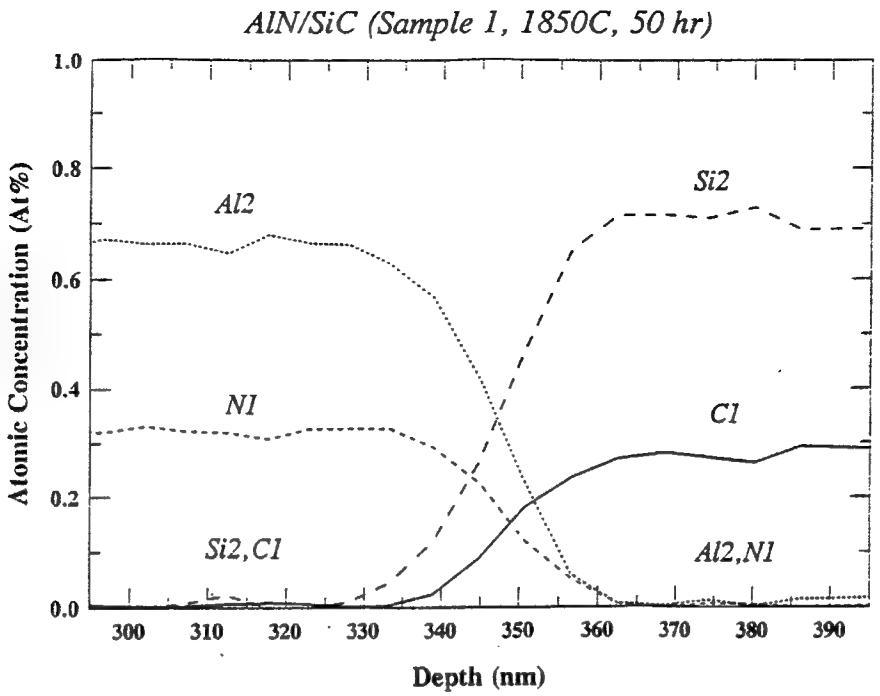


Figure 1. Auger depth profile of sample 1.

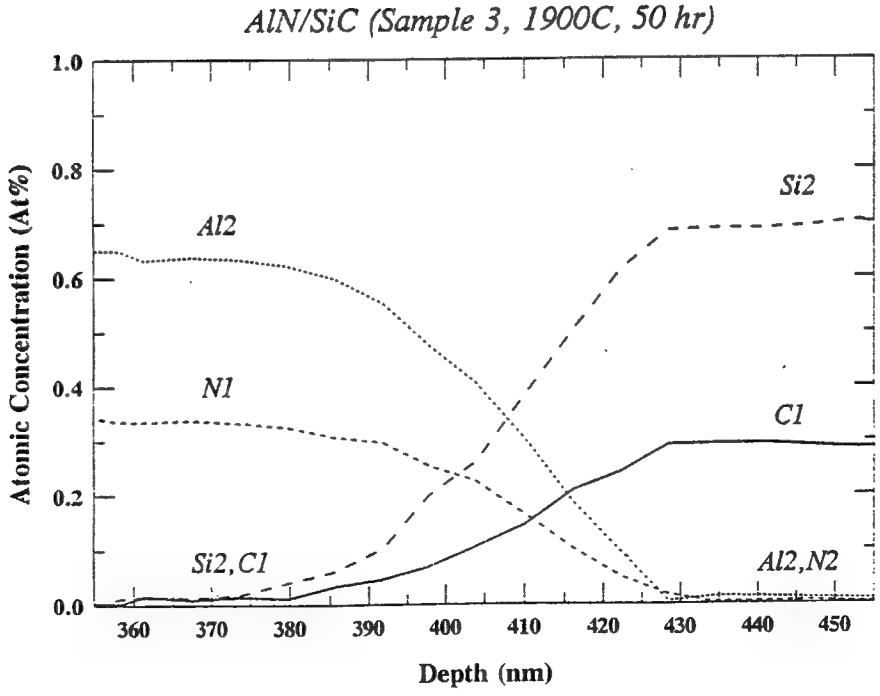


Figure 2. Auger depth profile of sample 3.

Table 4. Parallel Electron Energy Loss Results Across the SiC/AlN Interface

| | | Intensity ($\times 10^{11}$) | | | | | |
|---|---|---|---|---|---|---|---|
| Position | Distance | Al | Si | N | C | Si/AI | C/N |
| | -70 | 0 | 2.14 | 0 | 0.93 | 0 | 0 |
| 2 | -60 | 0.09 | 2.21 | 0 | 1.00 | 24.6 | 0 |
| 3 | -50 | 0.08 | 2.51 | 0 | 1.04 | 31.4 | 0 |
| 4 | -40 | 0 | 2.33 | 0 | 1.04 | 0 | 0 |
| 5 | -30 | 0.02 | 2.23 | 0 | 1.03 | 11.5 | 0 |
| 6 | -20 | 0.17 | 2.02 | 0 | 1.02 | 13.1 | 0 |
| 7 | -10 | 0.36 | 1.95 | 0.08 | 0.87 | 5.41 | 10.88 |
| 8 Interface | 0 | 1.1 0 | 1.49 | 0.05 | 0.48 | 1.35 | 0.096 |
| 9 | 10 | 1.85 | 0.96 | 0.91 | 0.07 | 0.51 | 0.077 |
| 10 | 20 | 2.19 | 0.58 | 1.11 | 0 | 0.26 | 0 |
| 11 | 30 | 2.24 | 0.38 | 1.12 | 0 | 0.17 | 0 |
| 12 | 40 | 2.34 | 0.28 | 1.12 | 0 | 0.12 | 0 |
| 13 | 50 | 2.63 | 0.22 | 1.22 | 0 | 0.08 | 0 |
| 14 | 60 | 2.57 | 0 | 1.23 | 0 | 0 | 0 |
| 15 | 70 | 2.66 | 0.30 | 1.28 | 0 | 0.11 | 0 |

From Auger depth profiles, the interface region (16 nm) of Sample 1 is slightly sharper than the interface region (29 nm) of Sample 3. However, these values are roughly equal to the interface resolution predicted from experimental conditions (15 nm) and are consistent with a well-defined interface. Parallel electron energy loss chemical analysis of the region around the interface verifies that no long range diffusion occurred in samples annealed within the range 1700°–1950°C. The smoothness of the concentration verses distance profiles of samples 1 and 3 in Figs. 1 and 2, respectively indicate that there are no two phase regions formed in samples annealed between 1700–1950° C. This supports the phase diagram presented by Zangvil and Ruh that solid solutions between AlN/SiC are at best very limited at T<2000° C.

D. References


1. G. Schneider, L. J.Gauckler and G. Petzow, Material Science Monographs **6**, 399 (1980).
2. R. Ruh, A. Zangvil, J. Am. Ceram. Soc. **65** [5], 260 (1982).

3. R. Ruh, A. Zangvil, J. Barlowe, Am. Ceram. Soc. B~ll. **64** [10], 1368 (1985).
4. A. Zangvil, R. Ruh, J. Am. Ceram. Soc., **71** 884 (1988).
5. W. Rafaniello, K. Cho, A. V. Virkar, Mater. Sci., **16** [12], 3479 (1981).
6. W. Rafaniello, M. R.Plichta, A. V.Virkar, J. Am. Ceram. Soc., **66** [4] 272 (1983).
7. I. B. Cutler, P. D .Miller, W. Rafaniello, H. K. Park, D. P. Thompson and K. H. Jack, Nature, **275** 434 (1978).
8. G. Sukhanek, Y. M. Tairov, V. F. Tsvetkov, Pis'ma Zh. Tekh. Fiz. **8** [12], 739 (1983).
9. M. Shimada, K. Sasaki, M. Koizumi, Proc. of Inter. Sym. on Ceram. Components for Engines (1983).
10. K. Tsukuma, M. Shimada, M. Koizumi, J. Mater. Sci. Lett. **1** 9, (1982).

# V. Design and Development of Multiple Quantum Well Vertical Cavity Surface Emitting Laser Structures Via Molecular Beam Epitaxy

## A. Introduction

Recent research efforts in the wide-bandgap, III-V nitride, semiconductor field have concentrated on the development of light-emitting diodes (LEDs) that emit in the blue spectral region. An AlGaN/InGaN/AlGaN double heterostructure blue LED has been developed in Japan and is now commercially available. The logical next step is the fabrication of blue and UV lasers. The III-V nitrides are most promising candidate materials for these devices because they possess three favorable characteristics: (1) they all have direct transition band structures, (2) their bandgap energies range from the deep UV (6.2 ev (AlN)) to the orange (2.8 ev (InN)) regions of the spectrum, and (3) they can be mixed to form solid solutions allowing for the tailoring of bandgap energies to specific wavelengths.

One of the promising optical devices ideally suited for fabrication using the III-V nitrides is the Vertical Cavity Surface Emitting Laser (VCSEL). VCSELs have significant advantages over edge-emitting lasers for optoelectronic communications. The laser beam emitted from the VCSEL propagates normal to the plane of the substrate, thereby making alignment for chip-to-chip communication much simpler. Additionally, the chip area occupied by a VCSEL is relatively small compared to one required by an edge-emitter [1]. One unique feature of these VCSELs is that both the central light-emitting active region and the outermost distributed Bragg reflectors (DBRs) which form the Fabry-Pérot cavity are all dimensionally defined in one integrated crystal growth sequence performed over the entire wafer using epitaxial techniques such as Molecular Beam Epitaxy (MBE), Gas Source Molecular Beam Epitaxy (GSMBE) and CBE [2]. Efficient performance of such a device requires both high-quality crystalline microstructures and precise control of layer thickness and alloy composition to obtain the highly reflective mirrors and to ensure that the Fabry-Pérot resonance is placed at the exact wavelength for lasing. A typical schematic of a VCSEL structure is shown below. By incorporating a strained MQW active region and by varying the compositional ratios of the group III elements (Al, Ga, and In), the emission wavelength can be tailored to emit in the UV, blue and blue-green spectra.

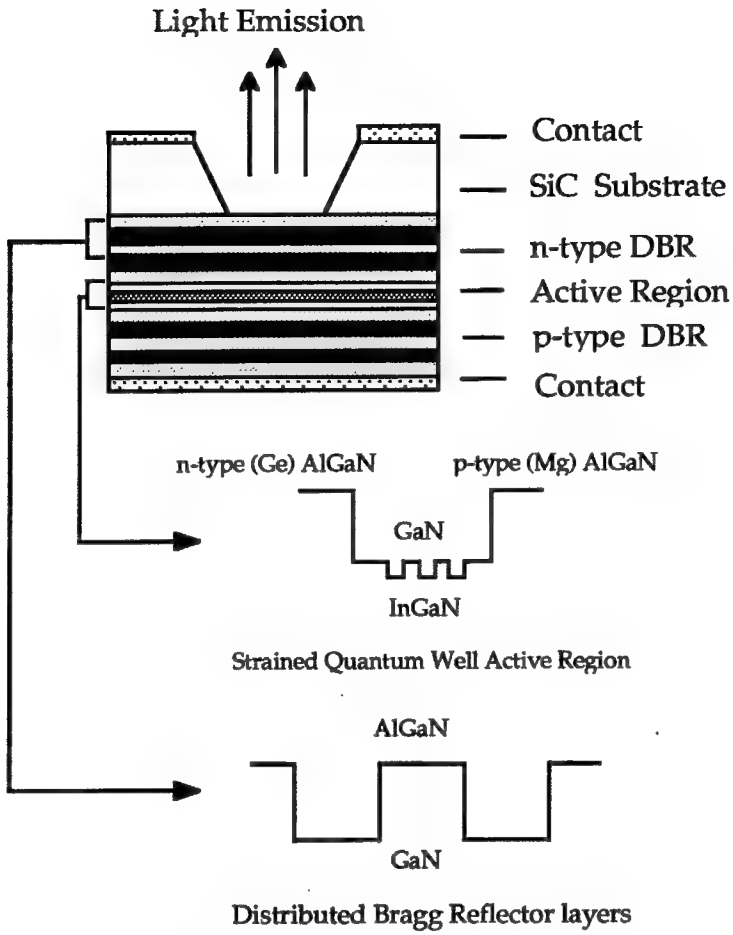


Schematic of a Typical VCSEL Structure

AlN, GaN and InN thin films are presently grown by various techniques including MOVPE, RF sputtering, and electron cyclotron resonance (ECR) plasma assisted GSMBE. Within the past several years, significant advances in GaN and AlN growth techniques have been achieved [3-12]. Consequently, high quality GaN epitaxial films that exhibit remarkably improved surface morphologies can now be produced by CVD growth techniques. We are currently employing GSMBE to determine the optimal growth parameters for the binary compounds, selected solid solutions of these compounds and multilayer heterostructures of these materials in terms of microstructure and optical and electrical properties. Additionally, researchers have successfully doped the III-V nitrides and their alloys creating n-type (Si, Ge) doped films [13-15] and more notably, p-type magnesium doped films [6,11,14]. Although these recent developments have provided all of the material ingredients necessary for the fabrication of efficient LEDs, further refinement in film quality, namely GaN and InN, is still needed for the GSMBE growth and fabrication of VCSEL structures. This report presents the

current research aimed at optimizing the microcrystalline quality of GaN by employing higher growth temperatures and buffer layer structures used in GaN thin-film growth.

B. Experimental Procedure

GaN thin-films were grown on (0001) oriented α(6H)-SiC wafers provided by Cree Research, Inc. The films were grown by ECR assisted GSMBE using a commercial Perkin-Elmer 430 system. The Al and Ga fluxes were provided by standard Knudson effusion cells. The $N_2$ source gas, ultra-high purity, was excited by an ECR plasma source. The ECR was designed to fit inside a standard effusion cell sleeve (2.25" diameter) [3]. All substrates were cleaned by a standard degreasing and RCA cleaning procedure prior to loading into the system. Additionally, the substrates were degassed at 700°C for 30 minutes prior to transferring to the deposition chamber.

Prior to depositing the GaN layers, either an AlN buffer layer or graded ($Al_xGa_{1-x}N$) buffer layer was deposited on the SiC surface. Compositional ratios of Al-atoms to the Ga-atoms in the $Al_xGa_{1-x}N$ buffer layers were varied through control of the Ga-cell, Al-cell, and substrate temperatures. Reflection high-energy electron diffraction (RHEED) was used to determine the crystalline quality of the films. Scanning electron microscopy (SEM) was used to analyze the films microstructures, and scanning Auger electron spectroscopy (AES) was used to determine the chemical composition of the graded buffer layers.

C. Results and Discussion

Figures 1 and 2 show the resulting microstructure of deposited GaN grown at 650° C using a low temperature (650° C) AlN buffer layer (250Å). The films were grown on 1) different polar planes of SiC (0001), namely the Si- and C-faces, and 2) different surface orientations, namely the on-axis and vicinal faces.

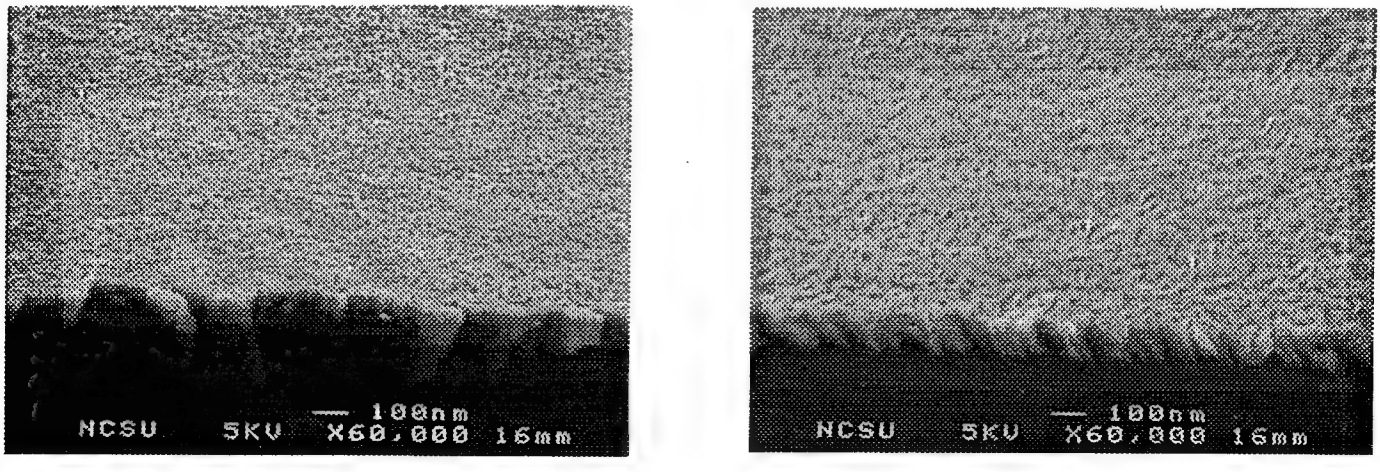


a) b)

Figure 1. Comparison of GaN grown on a) on-axis Si-face, and b) vicinal Si-face substrates.

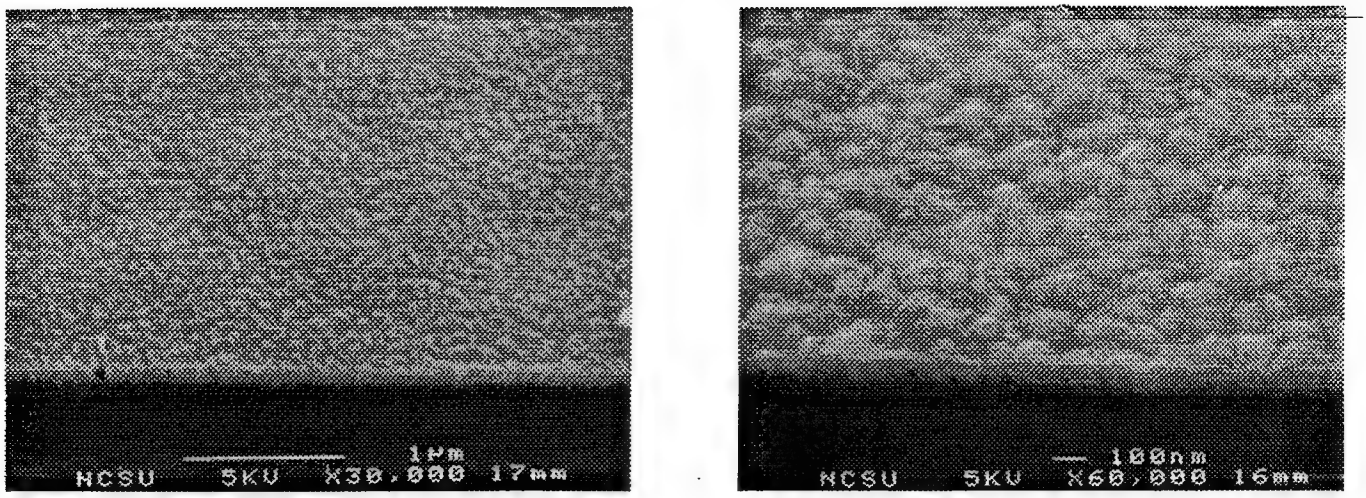


a) b)

Figure 2. Comparison of GaN grown on a) on-axis C-face, and b) vicinal C-face substrates.

We have reported earlier [16] that the quality of AlN films can be improved by incorporating the use of on-axis SiC (0001) substrates. By improving the quality of the AlN buffer, we expected the quality of the subsequent GaN films to also improve. Additionally, based on the results of work performed on films grown by OMVPE [17], a comparison of films grown on the Si- and C-faces was performed. Analysis of Figs. 1 and 2 reveals that the films grown on the different polar faces have quite dissimilar surface morphologies. SEM image analysis of the on-axis faces reveals smoother surface morphologies, however it is difficult to determine if an apparent reduction of columnar growth in the GaN layers was achieved. Further analysis by TEM may be used in the future to determine this issue.

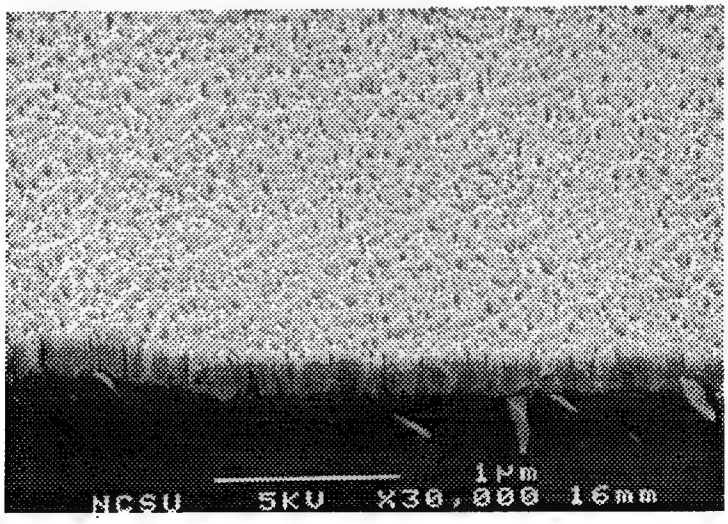


Figure 3. GaN grown at 750° C using an AlN buffer layer and the on-axis $(0001)_{Si}$ face.

Figures 3 and 4 show the result of increasing the growth temperature of the GaN film. A high temperature (1100°C) AlN buffer layer was used in this study. Figure 3 shows GaN deposited at 750° C, and Fig. 4 shows GaN deposited at 825° C. Analysis of these SEM images reveals that a smoother surface morphology and microstructure is obtained at the higher growth temperature.

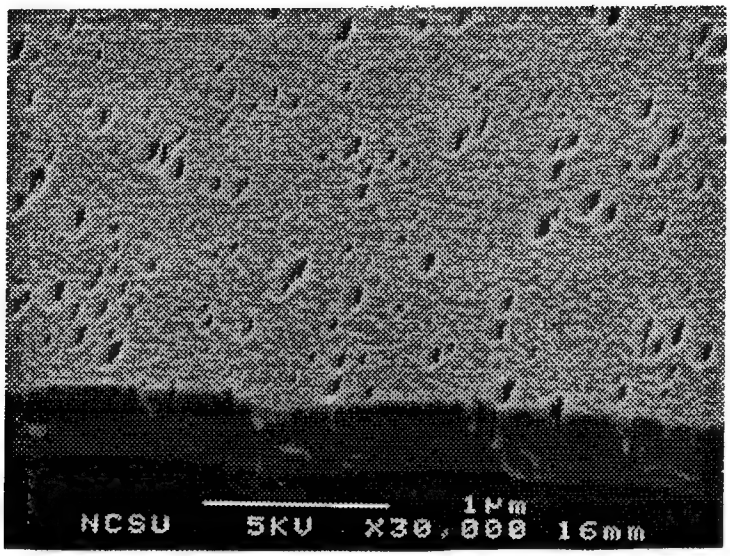


Figure 4. GaN grown at 825° C using an AlN buffer layer and the on-axis $(0001)_{Si}$ face.

Figure 5 shows the comparison of two different types of graded buffer layers used prior to the GaN deposition. Development of a graded buffer layer should result in a reduction of strain energy arising from the lattice mismatch between AlN (3.112Å) and GaN (3.189Å). This should aid in improvement of the resulting GaN film microstructure. Figures 5 (a) and 5 (b) show the deposition conditions used for the buffer growth. Figures 5 (c) and 5 (d) show the resulting AES analysis of the films chemical compositions. Figures 5 (e) and 5 (f) show the resulting film microstructures. Analysis of the SEM images reveals two resulting primary differences between the buffer layers used. Firstly, in sample A, there is no clear distinction between the buffer layer and the subsequent GaN layer. However in sample B, an abrupt interface can be seen separating the graded buffer layer and the GaN layer. Secondly, There is a drastic reduction of columnar growth in sample A, whereas sample B still exhibits a high columnar density. It is surmised that the rate of compositional change of the buffer layer in sample B is most likely responsible for the poorer microstructure of the resulting film. Further refinement of the buffer layer deposition technique should result in a further improvement of film quality beyond that of sample A.

Sample A

Sample B

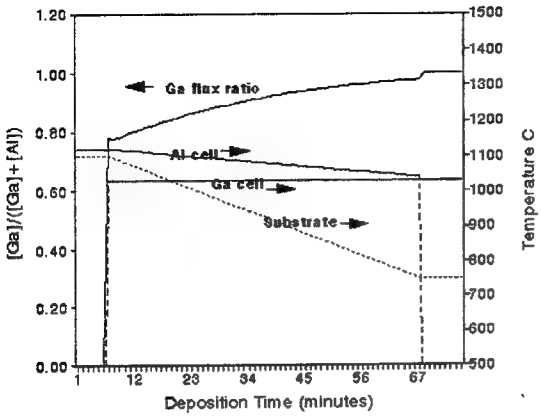


a)

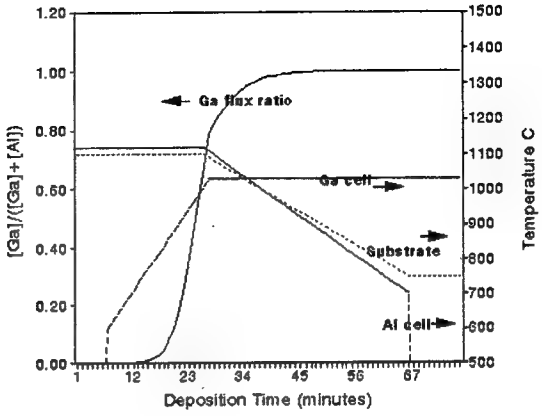


b)

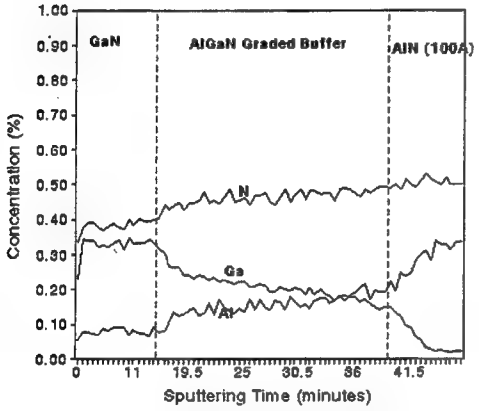


c)

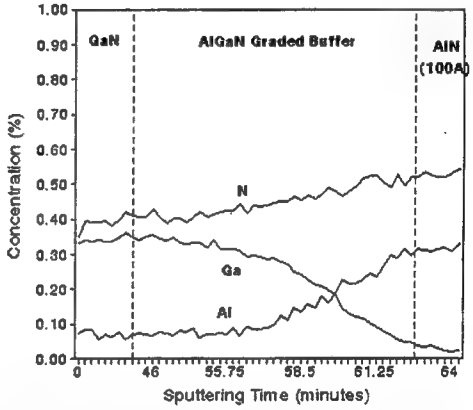


d)

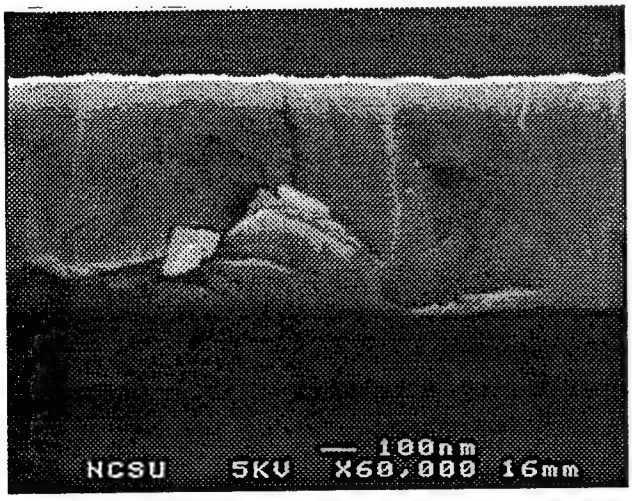


e)

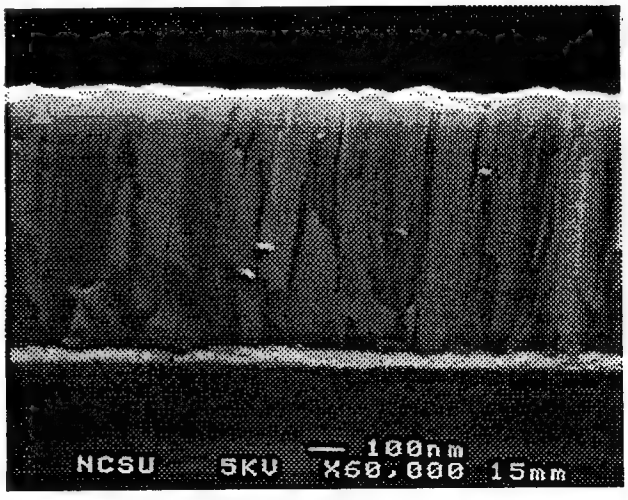


f)

Figure 5. a) and b) Growth parameters; c) and d) AES analysis; e) and f) SEM analysis.

D. Conclusions

GaN thin films were deposited on vicinal and on-axis, Si- and C-face 6H-SiC (0001) substrates using a low temperature buffer layer. Growth on the on-axis $(0001)_{Si}$ face resulted in the best surface morphology. The microstructural quality of GaN improves for films deposited at higher growth temperatures using a high temperature AlN buffer layer. The quality of GaN films grown on graded (AlGaN) buffer layers improves as the rate-of-change of the buffer composition is decreased.

E. Future Research Plans and Goals

Further improvement of GaN film quality will be studied by continuing to increase the deposition temperature of the GaN. At increased temperatures, the rate of desorption of the deposited Ga is expected to increase, and a limit will be reached where any gains in the quality of the film microstructure will be outweighed by a reduction of the resulting GaN film growth rate. Refinement of depositing a graded AlGaN buffer layer will also be investigated to aid in optimization of the GaN microstructure.

After optimizing the GaN film growth technique by GSMBE, we will begin studies aimed at precise in-situ film thickness monitoring. This will be necessary for fabrication of the Fabry-Pérot cavity and DBR mirrors necessary for efficient lasing of the VCSEL structures.

F. References


1. T. Miyamoto, T. Uchida, N. Yokouchi and K. Iga, J. Crystal Growth 136 (1994) 210
2. Y. M. Houng, M.R.T. Tan, B. W. Liang, S. Y. Wang, L.Yang and D. E. Mars, J. Crystal Growth 136 (1994) 216
3. Z. Sitar, M. J. Paisley, D. K. Smith and R. F. Davis, Rev. Sci. Instrum. **61**, 2407 (1990).
4. K. Hirosawa, K. Hiramatsu, N. Sawaki and I. Akasaki, Jpn. J. Appl. Phys. **32**, L1039 (1993).
5. S. Yoshida, S. Misawa and S. Gonda, J. Appl. Phys. **53**, 6844 (1982).
6. C. Wang and R. F. Davis, Appl. Phys. Lett. **63**, 990 (1993).
7. S. Nakamura and T. Mukai, Jpn. J. Appl. Phys. **31**, L1457 (1992).
8. T. Nagatomo, T. Kuboyama, H. Minamino and O. Omoto, Jpn. J. Appl. Phys. **28**, L1334 (1989).
9. M. A. Khan, J. M. Van Hove, J. N. Kuznia and D. T. Olson, Appl. Phys. Lett. **58**, 2408 (1991).
10. N. Yoshimoto, T. Matsuoka, T. Sasaki and A. Katsui, Appl. Phys. Lett. **59**, 2251 (1991).
11. S. Nakamura, M. Senoh and T. Mukai, Jpn. J. Appl. Phys. **30**, L1708 (1991).
12. J. Sumakeris, Z. Sitar, K. S. Ailey-Trent, K. L. More and R. F. Davis, Thin Solid Films **225**, 244 (1993).
13. S. Nakamura, P. Mukai, M. Senoh, Jpn. J. Appl. Phys. **31**, L139 (1992).
14. I. Akasaki, H. Amano, N. Koide, M. Kotaki and K. Manabe, Physica B **185**, 428 (1993).
15. N. Koide, H. Kato, M. Sassa, S. Yamasaki, K. Manabe, M. Hashimoto, H. Amano, K. Hiramatsu and I. Akasaki, J. Crystal Growth **115**, 639 (1991).
16. Semiannual Technical Report, Grant #N00014-90-J-1427.
17. Semiannual Technical Report, Grant #N00014-92-J-1720.

## VI. Deposition of Gallium Nitride via Supersonic Jets

I. Introduction

The nitride family of materials, GaN, AlN and InN as well as their solid solutions offer the possibility of new high-power and high-temperature devices. These materials have direct band gaps of 3.4, 6.28 and 1.95 eV, respectively. They form solid solutions with each other offering a wide range of possible band gaps [1]. GaN has a high electron drift velocity and would be suitable for high-frequency and microwave devices [1,2]. However, considerable efforts have been guided toward obtaining p-type or insulating GaN [2,3]. Glaser *et al.* [4] proposed a model based on native N vacancies to explain the n-type nature of GaN. To minimize the concentration of N vacancies, low temperature growth methods have been pursued. These methods include electron cyclotron resonance (ECR) microwave-plasma assisted molecular beam epitaxy, atomic layer epitaxy, ECR plasma enhanced metal organic vapor phase epitaxy and reactive magnetron sputtering [1,3,5-7]. The use of low temperature processes has also been reported to produce films with improved surface morphology [5]. Newman *et al.* proposed that the growth of GaN at low temperatures proceeds as a metastable process. Activated N species are required to overcome the kinetic barrier for GaN formation. The formation of GaN is controlled by the arrival of activated N species to the substrate surface. The decomposition of GaN is hindered by a large kinetic barrier [7]. $NH_3$ and $N_2$ are the most common N sources utilized for GaN film growth [1,6,8,9]. $NH_3$ can be decomposed thermally at substrate temperatures of 600°C to produce NH radicals which adsorb onto the substrate [8]. $N_2$ is used with the assistance of a plasma source to produce activated N species. This allows GaN to grow at substrate temperatures as low as 450°C [9].

In the present project we propose to use Supersonic Jet Deposition (SJD) to grow GaN. In SJD a diluted mixture of a gas phase Ga precursor and a N precursor are expanded through a small (≈100μm) orifice from a high pressure reservoir ($P_o$) into a low pressure chamber ($P_b$). The expansion of the gas reduces the temperature of the gas and therefore the enthalpy of the molecules. If the ratio ($P_o/P_b$) is greater than 2 the expanded species will attain an average velocity equal to the speed of sound. This is due to the conversion of the thermal energy or enthalpy of the species in the reservoir into directed kinetic energy. The ultimate velocity V, that the species will attain depends on the reservoir temperature $T_o$, and the molecular weight of the gas W, by the following equation [10]:

$$V = M\sqrt{\frac{\Omega R T_o}{W}}\left[1+\frac{\Omega-1}{2}\right]^{\frac{-\Omega}{\Omega-1}}$$

where Ω is the ratio of the heat capacities at constant pressure and volume, R is the universal gas constant, and M is the Mach number. M is a measure of the conversion of enthalpy into

kinetic energy [11]. If the carrier gas used to dilute the precursors is lighter than the precursors, during the expansion the heavier species attain the velocity of the lighter species [10]. This occurs because of elastic collisions between the gas molecules during the expansion. The variation of temperatures, carrier gases and precursors allows for the generation of activated species with kinetic energies ranging from 0.1 to 20 eV [10,12].

During the supersonic expansion a mach disk is formed at a distance dependent on $P_o/P_b$ via the following equation [10]:

$$\frac{X_m}{d} = 0.67\left[\frac{P_o}{P_b}\right]^{\frac{1}{2}}$$

where $X_m$ is the mach disk distance from the nozzle, and d is the nozzle diameter. During free jet deposition it is important however that the sample be within the mach distance such that the molecules have a high kinetic energy.

Ceyer (13) studied the effect of kinetic energy on the dissociative chemisorption of $CH_4$ on Ni (111) substrates. It was shown that the probability for dissociative chemisorption of $CH_4$ increased linearly with increase in translational energy of the molecule. This was correlated to the distortion of the C-H bonds upon collision of $CH_4$ onto the substrate. At high kinetic energies the deformation of the bonds allows the C atom sees the surface and a CH radical adsorbs giving off H atoms. Eres and Sharp [14] showed that Ge deposited on Ge (100) substrates was a result of a chemisorption reaction. They also found that growth of subsequent layers was controlled by the desorption of H from the adsorbed Ge.

Si and Ge have been deposited using supersonic jets. Eres *et al.* deposited Ge on GaAs by pulsed SJD [15]. The pulsed mode of SJD follows the same principles previously explained, but the nozzle is opened for short time intervals and then closed creating pulses of gas. Eres *et al.* used digermane ($Ge_2H_6$) as a precursor and He as a diluent. They observed very high epitaxial growth rates (0.25 μm/s), two orders of magnitude higher than in CVD at the same temperatures. They also estimated that 75% of the digermane came in contact with the substrate. The film growth efficiency was calculated to be 0.01 [15]. In another study Eres *et al.* showed that the crystallinity of the film could be controlled by SJD to give amorphous films at very high deposition rates [16]. This is in agreement with kinetics as the growth rate of Ge is a function of the arrival rate and decomposition rate of $Ge_2H_6$ on the GaAs. Under low $Ge_2H_6$ exposures, the deposited Ge is allowed to diffuse along the surface and form a highly crystalline structure. At high fluxes the arrival rate prevents the atoms from diffusing along the surface to form a crystalline structure and therefore a amorphous structure is developed.

Ohmi *et al.* [17] grew homoepitaxial Si films at growth rates of 0.5 μm/min. Films with low defect concentrations and little contamination were obtained at temperatures as low as

600°C . The growth mechanism was found to be dominated by the chemical decomposition on the surface of the substrate. Disilane ($Si_2H_6$) was used as a precursor. Zhang *et al.* [18] grew GaAs by a pulsed mode SJD. Trimethyll gallium (TMG) was used as the Ga precursor. The substrate was continuously exposed to $AsH_4$. The epitaxial growth was controlled by adjusting the TMG source pulse width. This provides a means to control the individual submonolayer growth.

The purpose of this study is to identify an operating window for the growth of GaN films via SJD using triethyllgallium (TEG) and ammonia ($NH_3$) as precursors. It is proposed that the surface decomposition of these precursors will be aided by the translational kinetic energy obtained during the expansion. The translational kinetic energy might also aid the surface diffusivity of the deposited species by the generation of surface phonons.

B. Experimental Procedure

Figure 1 is a schematic of the SJD unit used to deposit GaN. The chamber is partitioned into two sections. The front section serves as a source chamber and is pumped by a diffusion pump (CVC PVMS-6) which is backed by a Tuthill 3206 roots blower and a Welch 1374 direct drive mechanical pump. The back chamber is pumped by a Varian VHS-6 diffusion pump backed by a Varian 2033 mechanical pump. A cold cathode and pirani sensor connected to a Leybold CC-3 gauge readout is used to monitor the pressure of the chamber. The base pressure of the system is 10E-7 torr. The sample is heated by a halogen lamp encapsulated in the sample stage. The samples are introduced into the chamber via a mechanically pumped load lock with a molecular sieve. The load lock is pumped to 1 mtorr before introducing the sample into the chamber.

Two separate nozzles are used to introduce the precursors. TEG (Air Products) is transported by flowing He through a metalorganic bubbler. The TEG flow was controlled by adjusting the bubbler temperature and carrier flow rate. The TEG nozzle consists of a 1/8" stainless steel tube with a 1mm orifice. The $NH_3$ (obtained from Matheson and further purified with a Pall Gaskleen metalorganic purifier) jet is composed of 96% He and 4% $NH_3$. The source is comprised of a 1/8" stainless steel tube with a screw on nozzle cap. This cap holds a Ni pinhole made by Electron Beam Sciences. The pinhole has and inside diameter of 200μm. A heating coil is wrapped around the $NH_3$ nozzle. This provides for a $NH_3$ jet of variable energy. The pressure of the $NH_3$ nozzle (1000 torr) is controlled using a MKS 127A Baratron guage which feeds back to a MKS 647 microprocessor based multichannel flow/pressure controller. The latter regulates the flow of the gasses through a MKS 1159 MFC. The gas products are removed using a 5 gallon Novapure activated charcoal cannister and vented through a chemical hood.

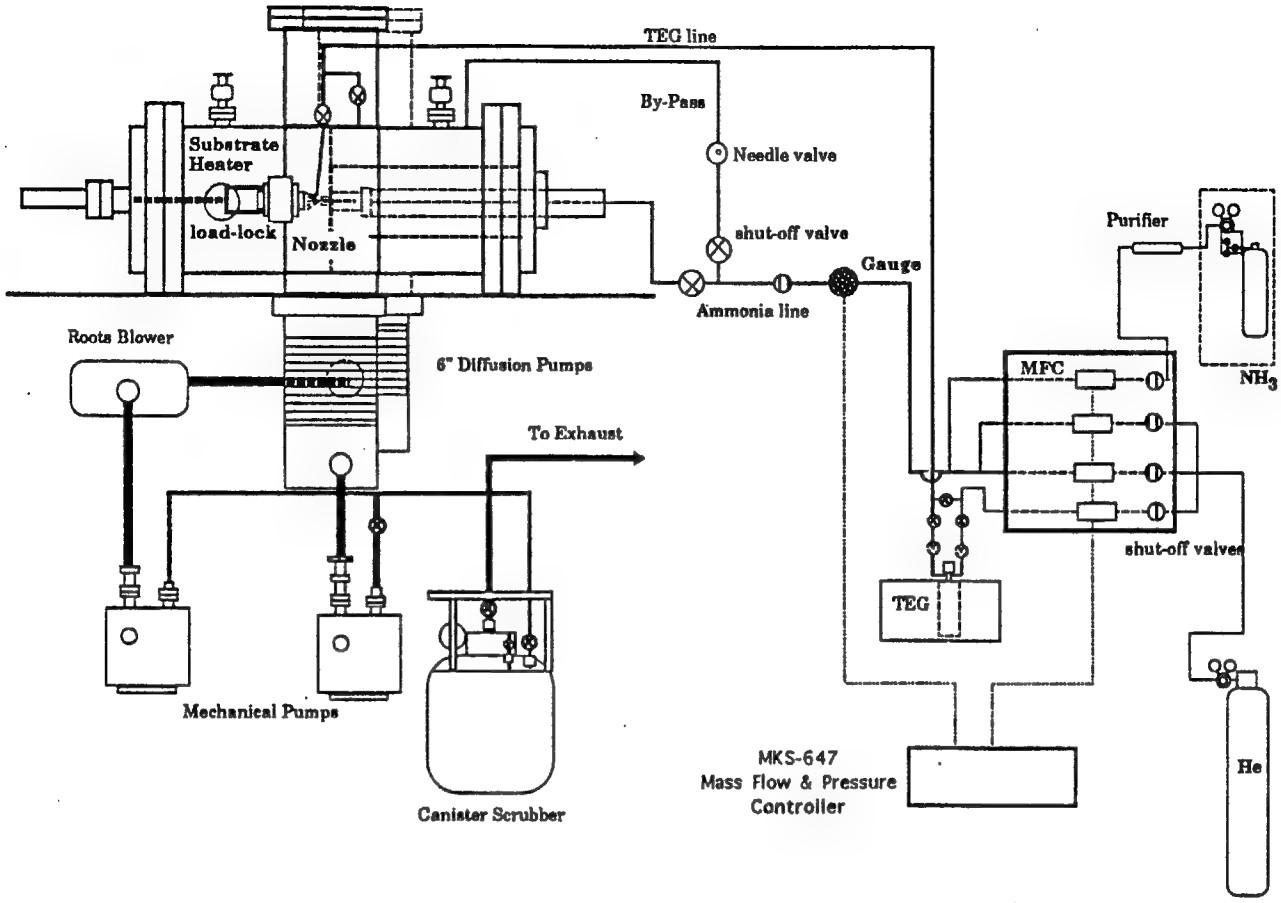


Figure 1. Dual supersonic jet deposition unit for deposition of GaN.

The GaN films were grown on sapphire (0001) substrates obtained from Crystal Systems. The substrates were degreased using 5 min. rinses in trichloroethylene, acetone, methanol and water. They were further cleaned by immersing in hot H3PO4:H2SO4 1:1 for 10 min., rinsed in deionized water for 10 min. and etched in 10% HF for 5 min. Films were grown under different gas compositions, substrate temperature and $NH_3$ nozzle temperatures. The growth of the films was characterized for composition, crystallinity and morphology using Auger Electron Spectroscopy (AES), X-ray diffraction (XRD) and Scanning Electron Microscopy (SEM) respectively.

C. Results

GaN films were grown at various $NH_3$:TEG ratios at a substrate temperature of 650°C and a nozzle temperature of 450°C. The $NH_3$ flow was kept constant (14 sccm) while the TEG flow was varied. Figure 2 shows the AES spectra obtained for the various $NH_3$:TEG ratios. Figure 3 shows the XRD pattern for GaN films grown at 650°C, $NH_3$ nozzle temperature of 510°C and a $NH_3$:TEG ratio of 730:1. Figure 4 shows the AES spectra for films grown at

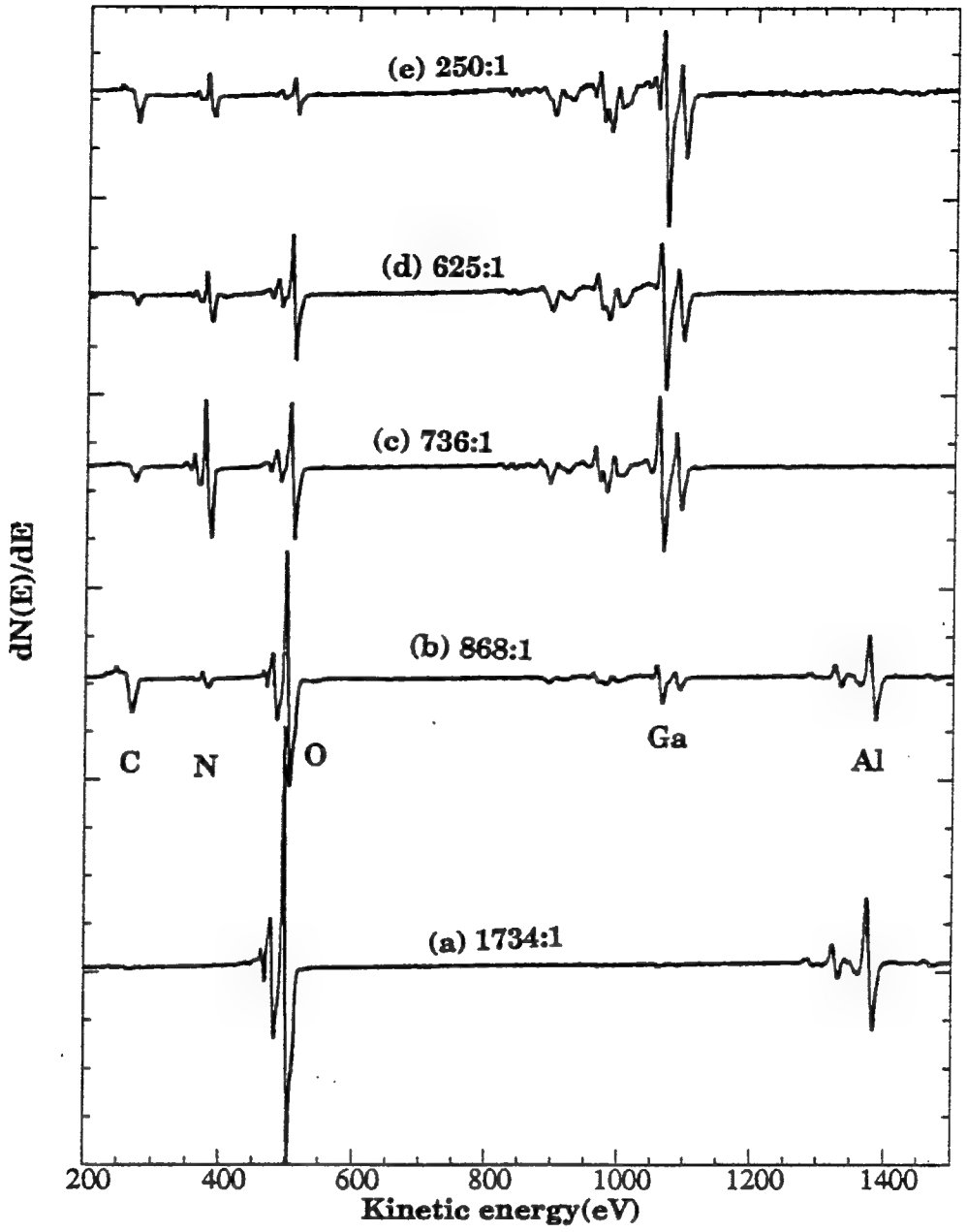


Figure 2. Auger electron spectroscopy of GaN films grown on sapphire (0001) at a substrate temperature of 650°C and nozzle temperature of 450°C.

various temperatures with a fixed $NH_3$:TEG ratio of 625:1. Figures 5-7 show SEM micrographs of GaN films grown at various nozzle temperatures. Growth of GaN was also obtained on Si (100) but Fe impurities were detected. These impurities were determined to proceed from the cleaning of the samples. The films showed very high growth rates (10μm/hr.). However, these results have been discarded since in the absence of the Fe impurities minimal growth was obtained. Fe has been identified as a catalyst for the synthesis of $NH_3$ and it's role in the growth of GaN is unknown.

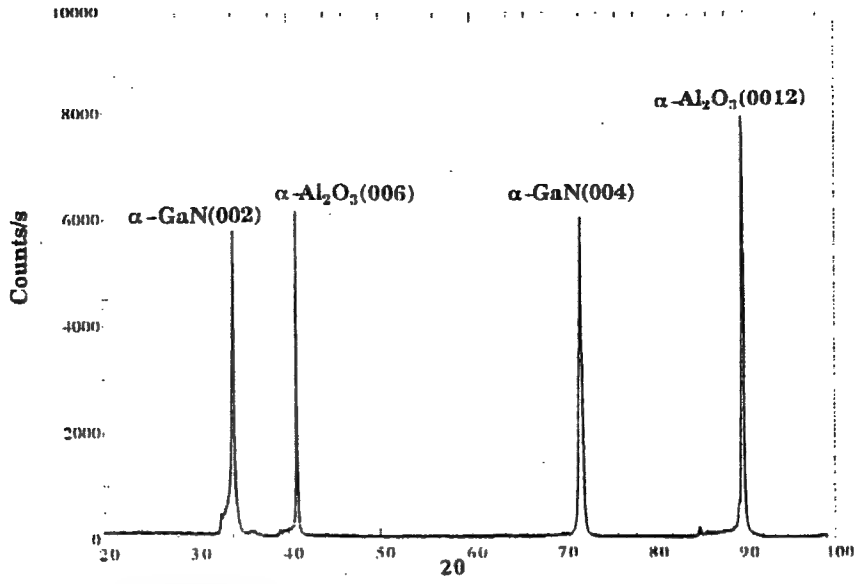


Figure 3. X-ray diffraction pattern for GaN films grown at 650°C, nozzle temperature of 510°C and $NH_3$:TEG = 730:1.

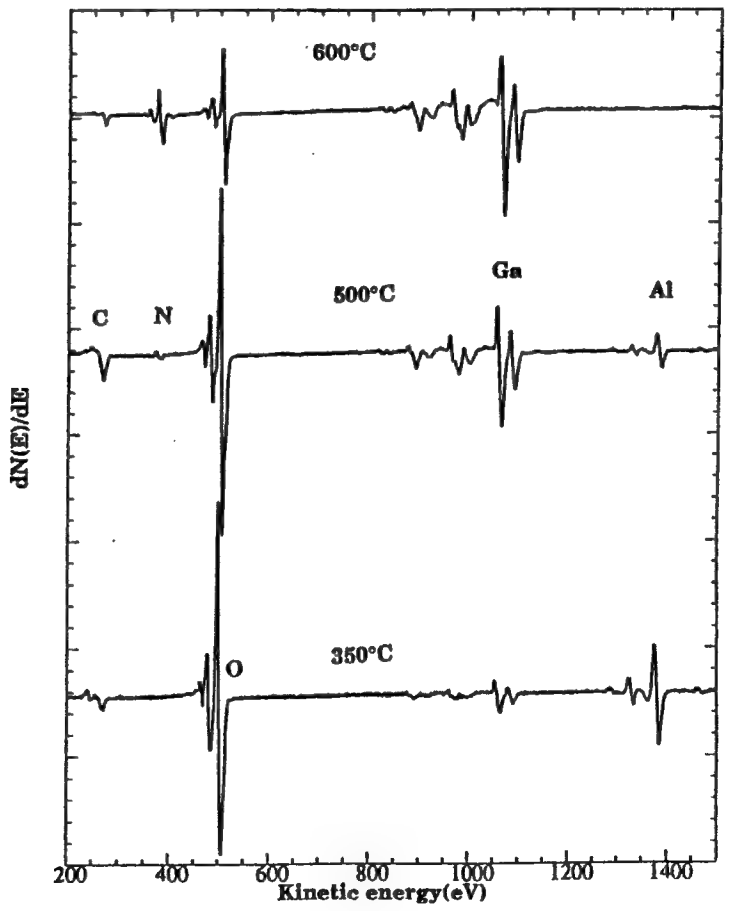


Figure 4. Auger electron spectroscopy of samples grown at various substrate temperature with a $NH_3$:TEG ratio of 625:1.

(a)

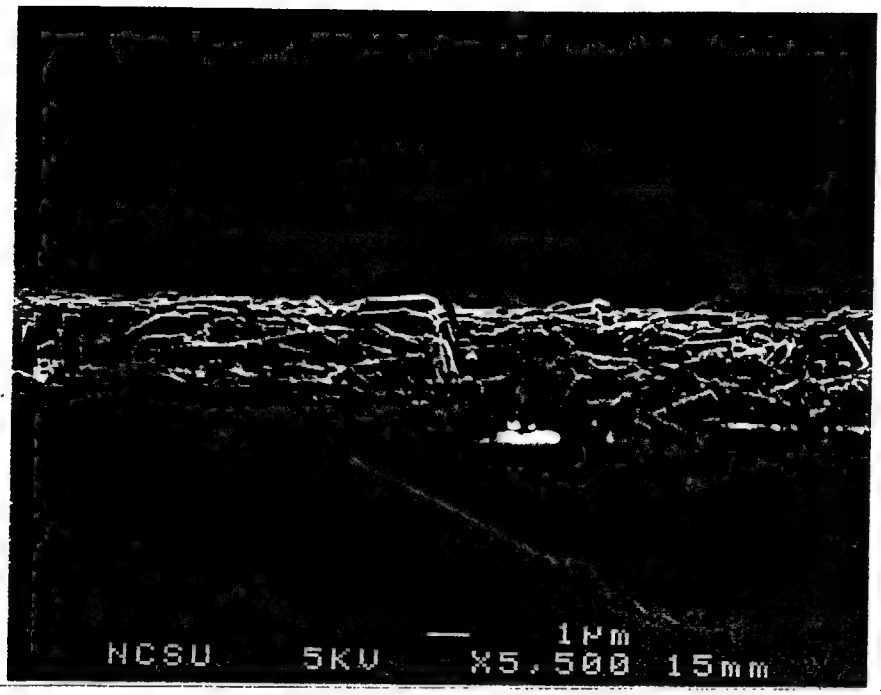


(b)

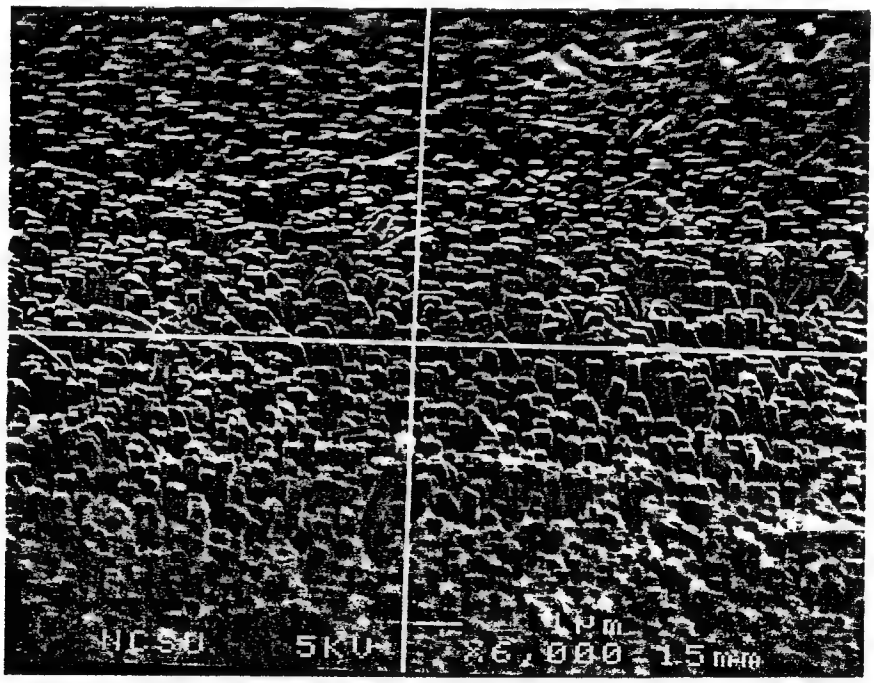


Figure 5. SEM of a GaN film grown at 650°C with a nozzle temperature of 510°C.

(a)

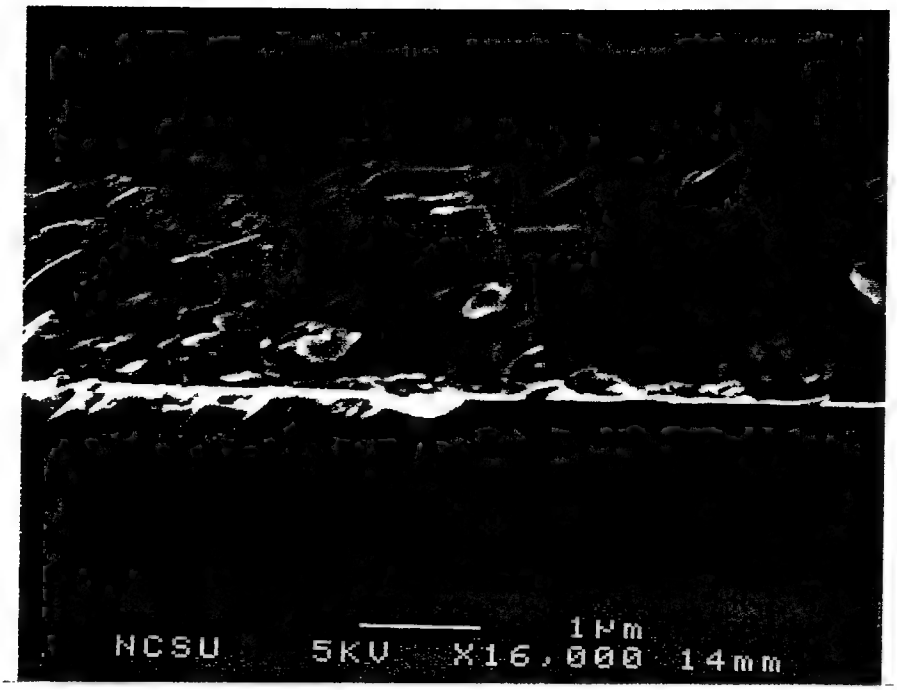


(b)

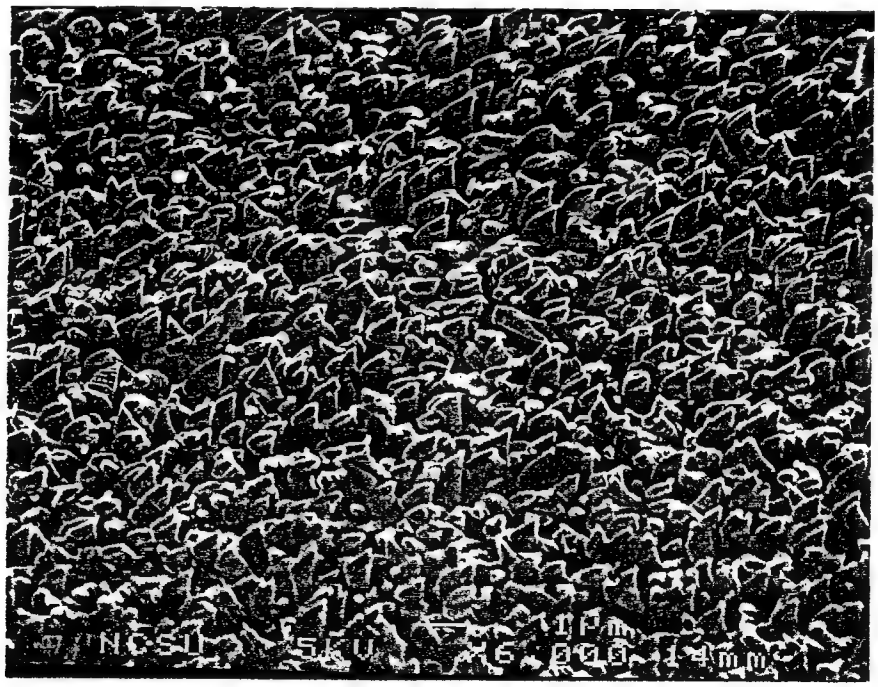


Figure 6. SEM of a GaN film grown at 650°C with a nozzle temperature of 400°C.

(a)

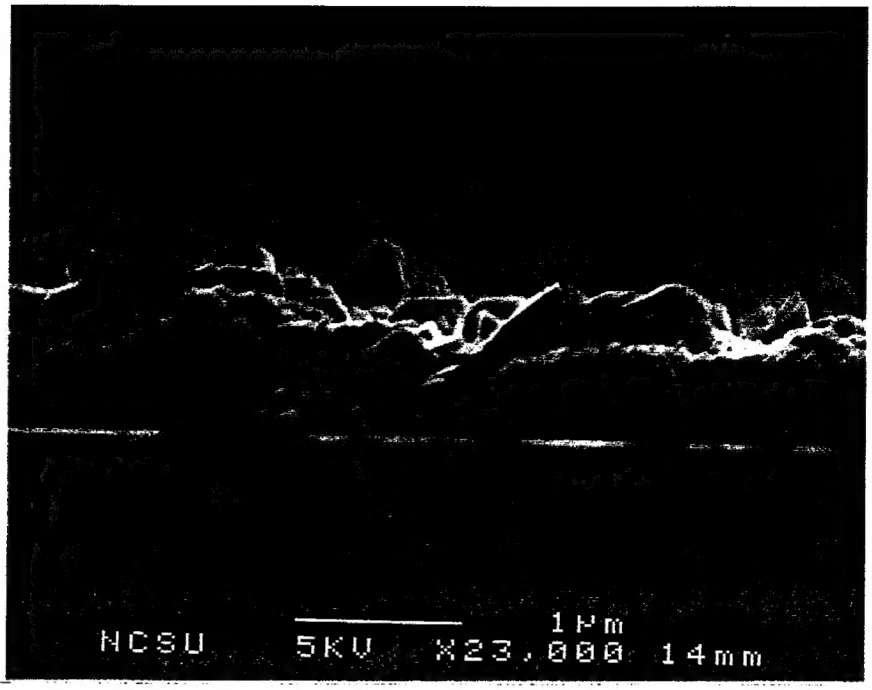


(b)

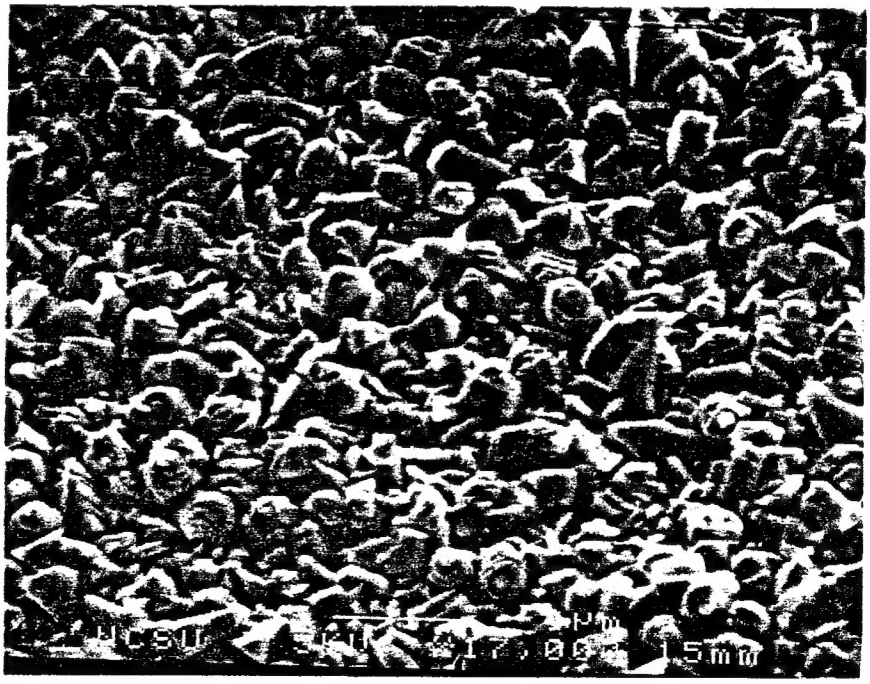

Figure 7. SEM of a GaN film grown at 650°C with a nozzle temperature of 90°C.

D. Discussion

Figure 2 shows the AES spectra obtained for the various NH3:Ga ratios used. No Ga or N are detected at ratios higher than 868:1. The Ga and N signals increase with decreasing ratio until the ratio is less than 600 where films are Ga rich due to insufficient $NH_3$. The trends observed suggest that the growth of GaN is controlled by the amount of Ga reaching the substrate. The deposition pressure is <10 mtorr which suggests that the process is not transport limited as is the case of MOCVD. The growth is then limited by the chemistry of the system. The main contaminants are C and O. These were picked up during exposure of the film to atmosphere.

Figure 3 shows the XRD pattern for GaN films grown at 650°C, $NH_3$ nozzle temperature of 510°C and a $NH_3$:TEG ratio of 730:1. The only reflections found correspond to wurtzite GaN and are due to the (002) and (004) reflections. This shows that the films were strongly oriented along the [001] direction suggesting an epitaxial relation between the sapphire (001) substrate and the film. Powell *et al.* (9) also identified this epitaxial relationship. They proposed a model where the film aligned with the substrates oxygen sublattice. And therefore it exhibits a 16% lattice mismatch.

Figure 4 shows the AES spectra for films grown at various substrate temperatures with a fixed $NH_3$:TEG ratio of 625:1. The Ga signal is minimal and no N signal is shown at 350°C. At 500°C and 600°C both signals increase. The N signal is found to increase slower due to a higher activation energy for the decomposition of $NH_3$. This suggests that the chemistry of the system in terms of decomposition temperature is fixed by $NH_3$. Therefore, as long as the conditions of deposition satisfy the conditions for the decomposition of $NH_3$ a film is deposited. The amount of material used in this process is much lower than that used in CVD and comparable growth rates are obtained. This suggest that the efficiency of this process is only limited by the amount of material used as long as $NH_3$ decomposes.

Figures 5-7 show SEM micrographs of films deposited at various nozzle temperatures (i.e. NH3 kinetic energy). The morphology of the films is that of columnar growth. This could be due to the rapid growth rates preventing the film from undergoing 2D growth. The column's width ranges from 0.2 to 0.7 μm. The interface between the film and the substrate becomes smoother as the nozzle temperature decreases. This could also be due to high growth rates. The film thickness showed a variation with nozzle temperature. At nozzle temperatures of 510°C, 400°C and 90°C the film thickness was 3.5 μm, 1.8 μm and 1μm. All films were grown for 45 min. This suggest that kinetic energy effectively enhances the decomposition of $NH_3$ and therefore the growth of GaN. However it is also possible that the high velocities attained by the $NH_3$ molecules increased the number of molecules reaching the substrate where the $NH_3$ decomposes. This would suggest that $NH_3$ jets with higher kinetic energies are required. But at high temperatures $NH_3$ will decompose into $N_2$ which won't chemisorb.

E. Conclusions

Highly oriented (001) wurtzite GaN films have been grown on sapphire (001) at temperature ranging from 500°C to 650°C using SJD. The film growth is controlled by the decomposition conditions of $NH_3$ and the arrival of TEG to the substrate. The films are of columnar morphology and exhibit growth rates as high as 4.5 μm/hr. Kinetic energy or a high $NH_3$ incident flux enhanced the growth rates of the films.

F. Future Plans and Goals

The SJD unit has been retrofitted to a single nozzle configuration. Preliminary results show that the temperature for film deposition on sapphire increases with this arrangement. However, growth on Si (100) has been observed to initiate at 650°C by AES. However at 750°C the films are highly contaminated by C. This could be due to high growth rates trapping the organic byproducts from TEG decomposition. The operating window for growth via this mode is to be identified. The system will then be upgraded to a triply differentially pumped system with several analytical tools such as XPS, RHEED, etc.

G. References


1. T. Lei, T. D. Moustakas, R. J. Graham, Y. He and S. J. Berkowitz, J. Appl. Phys., **71**(10), 4933 (1992).
2. M. J. Paisley, Z. Sitar, J. B. Posthill and R. F. Davis, J. Vac. Sci. Technol. **A7** (3) (1989).
3. C. Wang and R. F. Davis, Appl. Phys. Lett. **63** (7), 990 (1993).
4. E. R. Glaser, T. A. Kennedy, J. A. Freitas Jr., M. Asif Khan, D. T. Olson and J. N. Kuznia, presented at the International Conference on Silicon Carbide and Related Materials ISCRM), Washington D.C. (1993)
5. S. Zembutsu, and T. Sasaki, Appl. Phys. Lett., **48** (13), 870 (198).
6. J. Sumakeris, Z. Sitar, K. S. Ailey-Trent, K. L. More and R. F. Davis, Thin Solid Films **225**, 244-249 (1993).
7. N. Newman, J. Ross and M. Rubin, Appl. Phys. Lett., **62**(11),1242 (1993).
8. R. C. Powell, N. E. Lee and J. E. Greene, Appl. Phys. Lett., 60(20), 2505 (1992).
9. R. C. Powell, N. E. Lee, Y. W. Kim and J. E. Greene, J. Appl. Phys., **73**(1), 189 (1993).
10. D. Eres, D. H. Lowndess and J. Z. Tischler, J. Vac. Sci. Technol. A **11**(5), 2463 (1993).
11. D. Eres, D. H. Lowndess, J. Z. Tischler, J. W. Sharp, T. E. Haynes and M. F. Chisholm, J. Appl. Phys., **67**(3), 1361 (1990).
12. T. Ohmi, M. Morita, T. Kochi, M. Kosugi, H. Kumagai amd M. Itoh, Appl. Phys. Lett., **52**(14), 1173 (1988).
13. S. Zhang, J. Cui, A. Tanaka, Y. Agoyagi, Appl. Phys. Lett. **64**(9), 1105 (1994).
14. S. T. Ceyre, J. D. Beckerle, M. B. Lee, S. L. Tamg, Q. Y. Yang and M. A. Hines, J. Vac. Sci. Technol. **A 5**(4), 501(1987).
15. D. Eres and J. W. Sharp, J. Vac. Sci. Technol. **A 11**(5), 2463 (1993).
16. Giancinto Scoles Ed., Atomic and Molecular Beam Methods Vol. 1, Oxford University Press, New York (1988).
17. R. Campargue, J. Phys. Chem. **88**, 4466-4474 (1984).
18. H. Haberland, U. Buck and M. Tolle, Rev. Sci. Instrum. **56** 9), 1712 (1985).

## VII. Distribution List

| | |
|---|---|
| Mr. Max Yoder<br>Office of Naval Research<br>Electronics Division, Code: 314<br>Ballston Tower One<br>800 N. Quincy Street<br>Arlington, VA 22217-5660 | 3 |
| Administrative Contracting Officer<br>Office of Naval Research<br>Regional Office Atlanta<br>101 Marietta Tower, Suite 2805<br>101 Marietta Street<br>Atlanta, GA 30332-0490 | 1 |
| Director, Naval Research Laboratory<br>ATTN: Code 2627<br>Washington, DC 20375 | 1 |
| Defense Technical Information Center<br>Bldg. 5, Cameron Station<br>Alexandria, VA 22314 | 4 |